

HALL EFFECT AND ELECTRICAL CONDUCTIVITY,
IN CASSITERITE CRYSTALS

By

EUGENE ELMER TOLLY

"

Bachelor of Science

Northwestern State College

Alva, Oklahoma

1959

Submitted to the Faculty of the Graduate School of
the Oklahoma State University
in partial fulfillment of the requirements
for the degree of
MASTER OF SCIENCE
February, 1962

Thesis
1960
74410
1960

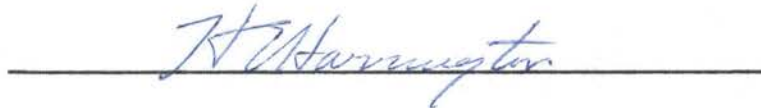
NOV 13 1962

HALL EFFECT AND ELECTRICAL CONDUCTIVITY
IN CASSITERITE CRYSTALS

Thesis Approved:



Thesis Adviser



Dean of the Graduate School

505279

This research was supported by the
Office of Naval Research under
Contract No. Nonr-2595(01)

ACKNOWLEDGMENT

The author wishes to express his gratitude in a very sincere thanks to all who have contributed to this effort, and particularly to Dr. E. E. Kohnke for his valuable guidance and for his forbearance when severe contact difficulties were encountered.

A special note of thanks goes to J. E. Hurt for his many helpful suggestions and discussions, and to H. Hall, F. Hargrove, and J. Shannon for the excellent work they did on the crystal holder and various apparatus components.

Financial aid through the Office of Naval Research is gratefully acknowledged.

TABLE OF CONTENTS

Chapter	Page
I. INTRODUCTION	1
II. THEORY	6
The Hall Effect	6
Units	10
Corrections to the Simple Theory.	11
General Conductivity Theory	15
III. APPARATUS, EXPERIMENTAL TECHNIQUES AND CRYSTALS.	21
The Crystal Holder.	21
The Circuit	29
Special Temperature Control Procedures.	33
Description of Samples.	36
Contacts	37
Preparation of Samples.	38
IV. RESULTS.	39
Summary	49
V. CONCLUSIONS AND SUGGESTIONS FOR FURTHER STUDY.	51
Perspective	51
Suggestions for Further Study	58
BIBLIOGRAPHY.	60

LIST OF TABLES

Table	Page
I. Crystal Dimensions	37
II. Measured and Calculated Values	50

LIST OF FIGURES

Figure	Page
1. The Hall Effect for Electrons.	9
2. Cross Section of Crystal Holder.	22
3. Crystal Holder Accessories	24
4. Cross Section of Assembly.	26
5. The Circuit.	30
6. Chopper Section and Cam.	34
7. Conductivity Data as a Function of Temperature	40
8. Hall Effect and Conductivity Data as a Function of Temperature for Sample IX.	42
9. Hall Effect and Conductivity Data as a Function of Temperature for Sample XIX	43
10. Hall Mobility as a Function of Temperature	45
11. High Temperature Conductivity (Foex)	47
12. Transmission Spectrum of Sample XIX.	48

CHAPTER I

INTRODUCTION

Hall effect and conductivity measurements yield considerable information about the conduction process in a semiconductor. The Hall effect by itself gives a measure of the sign and density of charge carriers in the conduction process. When conductivity measurements are also taken a calculation of the mobility and drift velocity of these carriers can be made. When readings are taken over a suitable temperature range, variations in the Hall coefficient and conductivity values can be used to determine characteristic activation energies in a sample. If intrinsic conduction is being observed, as may be the case in nearly pure samples at elevated temperatures, the activation energy value is a measure of the forbidden energy gap in the material being studied. At lower temperatures, or for less pure samples, this energy provides a measure of the impurity ionization energy.

The objectives of the present investigation were to design and obtain suitable apparatus for taking simultaneous Hall effect and conductivity measurements on natural cassiterite crystals over a range of temperatures extending from the liquid nitrogen point up to 500° K, to study the resulting data in view of previous work, and to consider possible implications.

Earlier studies of the electrical properties of cassiterite in this vein are limited--being confined mostly to thin films, sintered samples,

and pressed powders of tin oxide. On the other hand, there has been a considerable amount of work done with oxides similar to cassiterite (stoichiometrically SnO_2) such as rutile (TiO_2) which has the same basic crystalline structure, and zinc oxide (ZnO) which has a different structure but many comparable electrical properties. One of the more interesting examples of this line of work has been reported by H. Rupprecht¹ who studied the effects of controlled impurity concentration in zinc oxide.

From work done with tin oxide films Bauer² and Fisher³ have reported values of the order of 10^{-2} ohm-cm for resistivity, 10^{-1} $\text{cm}^3/\text{amp-sec}$ for Hall coefficients, $6 \text{ cm}^2/\text{volt-sec}$ for Hall mobilities, and 10^{20} cm^{-3} for electron concentration. Bauer reported activation energies of 0.02 eV (electron volts) near 100°K , and 0.05 eV near room temperature. Ishiguro and co-workers⁴ also studied films and have reported values of the order of 10^{-2} ohm-cm, 15-35 $\text{cm}^2/\text{volt-sec}$, and 10^{19} to 10^{20} cm^{-3} , for resistivity, mobility, and electron concentration, respectively.

LeBlanc and Sachse⁵ have reported resistivities for sintered samples around 10^8 ohm-cm at room temperature, and Guillery,⁶ who studied both powders and sintered samples, has reported values from 10^4 to 10^8 ohm-cm at low temperatures.

Aitchison⁷ has studied the properties of tin oxide films which he prepared on pyrex glass substrates by the hydrolysis of stannic chloride at temperatures between 500°C and 800°C . The approximate reaction is given by:



He found that adding indium oxide (In_2O_3) to the stannic chloride

solution caused a net increase in the film resistance, and adding penta-valent elements such as antimony (in the oxide form Sb_2O_5) decreased the resistance. Recording resistivity values from 1.6×10^{-2} to 9.15×10^{-2} ohm-cm for films and 3.6×10^8 ohm-cm for a natural cassiterite sample, he concluded that the low film resistivities were due to a stoichiometric excess of tin, or to oxygen vacancies. The increase in film resistance for doped samples was attributed to a compensating effect between the In^{3+} ions and the O^{2-} ions, whereas the opposite effect could be explained by considering the Sb^{5+} ions as donors.

Films prepared by the pyrolytic decomposition of the chlorides SnCl_2 and SnCl_4 have also been studied by Miloslavskii.⁸ Their properties were found to be much the same whether glass, quartz, mica, or rock salt was used as a substrate. Ionization energies quoted from conductivity data for the temperature range 150°C to 200°C were ~ 0.12 ev for samples with room temperature conductivities from 10^2 to 10^3 (ohm-cm)⁻¹ and electron densities from 10^{19} to 10^{20} cm⁻³, while optical transmission studies gave values ~ 0.15 ev. The temperature range of investigation was from -150°C to 300°C . When samples were heated above 350°C the conductivity measurements would not reproduce. Samples with room temperature conductivities from 10 to 100 (ohm-cm)⁻¹, he reports, failed to follow an exponential law. Conductivities below 105°C were found to vary only slightly, but with a negative temperature coefficient.

A later report on the same type materials gave comparable values for conductivities and electron densities.⁹ Hall effect measurements in an investigation range from 20°C to 300°C showed little or no temperature dependence in the Hall coefficient, while a slight but definite

increase in conductivities was observed. A plausible interpretation--based on impurity band conduction--was given for these characteristics. Hall mobilities were mostly $\sim 10 \text{ cm}^2/\text{volt-sec}$. The temperature dependence of conductivity disappeared in samples doped with antimony. Doping was found to be accompanied by increased conductivities similar to the results obtained by Aitchison.

Possibly the best--above room temperature--correlation that can be made with the values from the present investigation is to those obtained by Foex.¹⁰ Using pressed samples of stannic oxide powders prepared by the oxidation of tin with nitric acid followed by a heat treatment in air at 1200°C , he obtained two linear sections on a logarithmic plot of conductivity versus $1/T$ in a temperature range from 20°C to 1200°C (see Figure 11, Chapter IV). Using a conductivity relation of the form of equation (35), Chapter II, the two values of ΔE are 0.77 ev nearest room temperature, and 4.0 ev in the higher temperature range. The first value, 0.77 ev , compares favorably with values obtained in the same temperature range from the natural samples studied here.

Earlier conductivity measurements on natural samples of cassiterite, taken locally, have been reported by Northrip.¹¹ He obtained conductivity values from three rather different samples. Two of these were cut from the same crystal. The first was cut from an opaque rust brown region, the second from a clear region. The third sample, he reports, was transparent but smoky. From these three specimens he obtained room temperature resistivity values of 2.4 to 4.2 ohm-cm , $2.4 \times 10^4 \text{ ohm-cm}$, and a value somewhat less than 1 ohm-cm , respectively.

There has also been a considerable amount of work done on optical transmission and photoconductive response of natural cassiterite in

previous portions of the project of which this study is a part. The results are far too numerous for a comprehensive summary here and the reader is best referred to the separate works^{11,12,13,14} where additional references are given. Optical energy gap values calculated from transmission curves for cassiterite, as reported by Belski,¹³ usually center around the value of 3.5 ev. A transmission curve, typical of the first three samples studied here, is shown in Figure 12 of Chapter IV.

CHAPTER II

THEORY

The Hall Effect

An electron moving under the simultaneous influence of electric and magnetic fields, in otherwise free space, is subjected to the net force

$$\vec{F}_0 = -q(\vec{E}_0 + \vec{v}_0 \times \vec{B}_0), \quad (1)$$

where $-q$ is the electronic charge, \vec{E}_0 the electric field, \vec{v}_0 the electron velocity, and B_0 is the magnetic flux density. Using Newton's second law of motion in conjunction with equation (1) the equation of motion for the electron can be obtained. When the fields are at right angles an electron originally at rest takes on a cycloidal path of motion which results in a net displacement at right angles to both fields with direction given by $-q(\vec{v}_0 \times \vec{B}_0)$.

No such simple description applies to the motion of an electron when other (and less simple) forces also apply. In crystals the motion is complicated by imperfections, impurity scattering, scattering by lattice vibrations, etc., and is limited by charge accumulation. However, equation (1) lends insight into the effect discovered by E. H. Hall¹⁵ in 1879. He found that a thin gold foil carrying a longitudinal current exhibited a transverse electromotive force when it was placed at right angles to a magnetic field. From measurements of this effect he

was able to conclude that the transverse field set up was proportional to the product of the magnetic field and the current density. This relation is currently expressed as

$$E_H = -RBJ \quad (2)$$

where E_H represents the transverse (or Hall) electric field, R is the Hall coefficient, B the magnetic flux density, and J the current density.

Two theories evolved from this discovery. The first and simplest can be described using a relation like equation (1). The second, necessary to explain effects not accounted for in the simple theory, rests on quantum mechanics. Both theories can be found in a number of texts. Shockley,¹⁶ for example, treats both the elementary and advanced cases and indicates correlations between the two. The simpler theory more readily lends itself to application, and it will be presented here. Basically both these theories apply to both electrons and holes in the conduction process. A somewhat general development will be given.

Assume that a crystal with rectangular cross-section and length considerably greater than its width, carrying a longitudinal current I_3 , is placed in a magnetic field; and assume that the crystal is so oriented that the magnetic field direction is at right angles to the crystal faces as in Figure 1. If these conditions are simultaneously satisfied, at that particular instant an effect similar to that described with equation (1) produces a displacement of charge toward one edge of the crystal that in turn generates a field limiting this charge displacement. A more quantitative description can be given as follows: Initially, the "average current carrier" that travels with drift velocity \vec{v} , will experience a force

$$\vec{F} = q(\vec{E} + \vec{v} \times \vec{B}) = qE_3\vec{i}_3 + qv_3B_1\vec{i}_2 \quad (3)$$

where \vec{i}_2 and \vec{i}_3 represent unit vectors along axes 2 and 3 of Figure 1, respectively. The component of force along direction 2

$$F_2\vec{i}_2 = qv_3B_1\vec{i}_2 \quad (4)$$

will produce a displacement of charge in that direction until a field generated by this displacement balances it; i.e., an equilibrium will be established when

$$F_2 \text{ (net)} = qE_2 + qv_3B_1 = 0 \quad (5)$$

The field E_2 in this case is the Hall field; the Hall voltage is given by

$$V_H = -E_H w = v_3 B_1 w \quad (6)$$

where w is the width of the crystal.

The form of equation (6) may be changed by using the expression for current density

$$J_3 = nqv_3 = I_3/wt \quad (7)$$

where n is the charge carrier density in the conduction process, and t is the crystal thickness. Eliminating v_3 between equations (6) and (7) yields

$$V_H = (1/nq)I_3B_1/t \quad (8)$$

or

$$V_H = (1/nq)J_3B_1w \quad (9)$$

Equations (2) and (9) are equivalent expressions, related by

$$R = (1/nq) \quad (10)$$

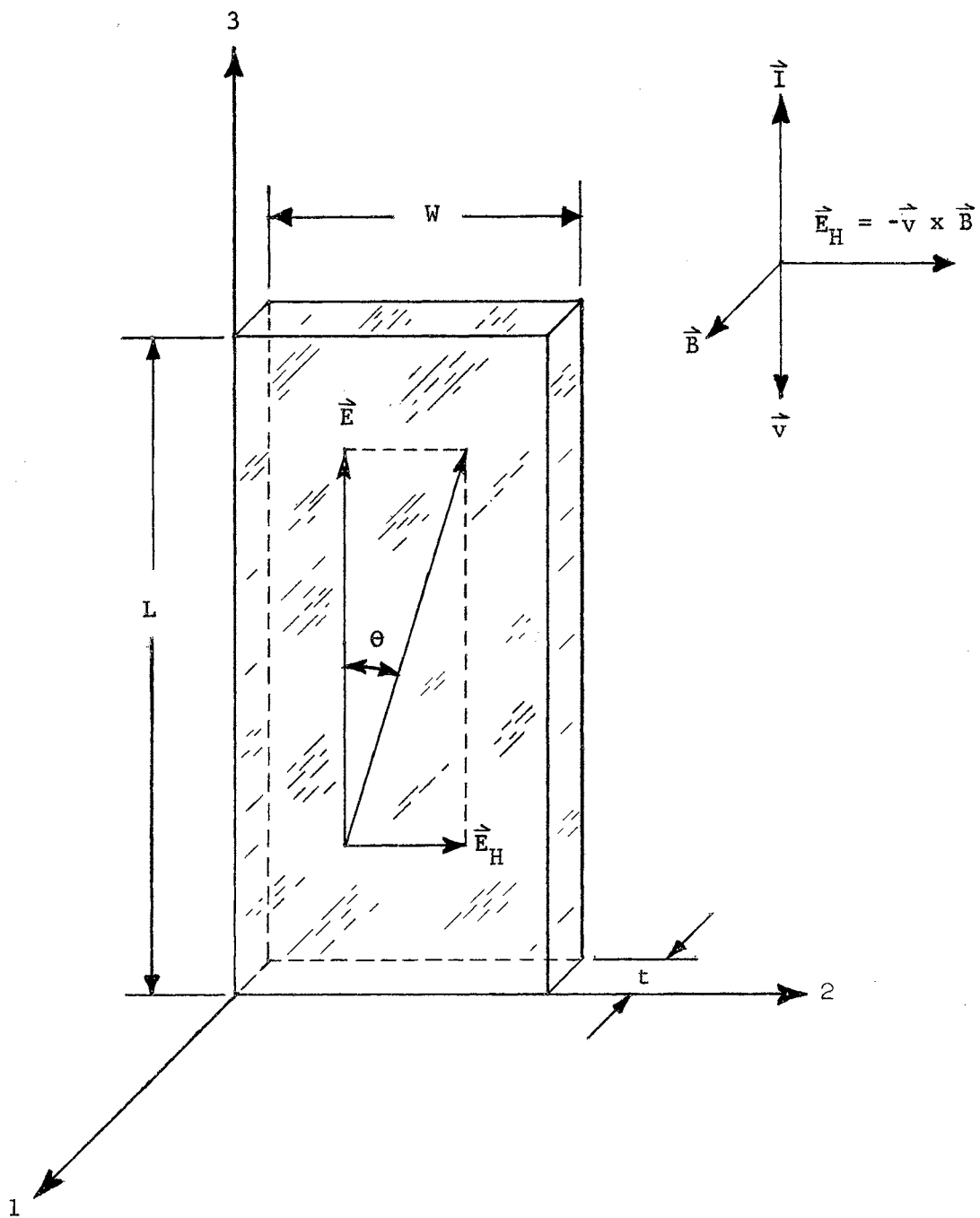


Figure 1. The Hall effect for electrons.

and equation (8) is another form of the same thing. Eliminating $(1/nq)$ between (8) and (10) results in

$$R = V_H t / I_3 B_1 \quad (11)$$

According to sign convention q will be negative for electrons and positive for holes. At the same time, if q is negative, v_3 will be negative, and hence J_3 of equation (7) will always be taken as positive. Similarly, V_H of equations (8), (9), and (11) will be negative for electrons as will R of (10) and (11). In the same way these equations can be applied to a system wherein holes dominate the conduction process, provided n is replaced by the symbol for holes (p), and both q and v_3 are taken as positive.

Units

Up to this point all equations have been expressed in the rationalized MKS system of units. It is desirable from the laboratory viewpoint to express these equations in terms of the units most commonly used in the current literature. Equation (8) has units of

$$(\text{meter}^3/\text{coulomb})(\text{ampere})(\text{weber}/\text{meter}^2)\text{meter}^{-1} = \text{weber}/\text{sec}$$

or volts. Noting that

$$1 \text{ weber}/\text{meter}^2 = 10^4 \text{ gauss}$$

and that

$$1 \text{ meter}^2 = 10^4 \text{ cm}^2$$

equation (8) can be transformed to

$$V_H = 10^{-8} (1/nq) IB/t \quad (12)$$

where the units are now:

$$\begin{array}{ll}
 V_H & \dots\dots\dots \text{volts} \\
 n & \dots\dots\dots \text{cm}^{-3} \\
 q & \dots\dots\dots \text{coulombs} \\
 I & \dots\dots\dots \text{amperes} \\
 B & \dots\dots\dots \text{gauss} \\
 t & \dots\dots\dots \text{cm.}
 \end{array} \tag{13}$$

Since the system of coordinate axes used is arbitrary the subscripts have been dropped in equation (12), and this will be done hereafter.

The Hall coefficient R will now be redefined as

$$R = 1/nq = 10^8 V_H t / IB \dots\dots \text{cm}^3/\text{coulomb.} \tag{14}$$

Future reference to any of these variables will imply units as in (13).

More generally, the system of units used are:

$$\begin{array}{ll}
 \text{Electrical} & \dots\dots\dots \text{ampere, coulomb, volt} \\
 \text{Magnetic} & \dots\dots\dots \text{gauss (or oersted)} \\
 \text{Mechanical} & \dots\dots\dots \text{centimeter, gram, second}
 \end{array}$$

Corrections to the Simple Theory

In general, mobility is defined by a relation of the form

$$\mu_q = v/E \tag{15}$$

where v is the drift velocity of current carriers produced by an electric field E . Direct determination of v for known values of E is possible in some cases by the injection of minority carriers into the conduction process of a sample. The details of this procedure are outlined by Shockley.¹⁶ Using equations (7) and (15), and the fact that

$J = \sigma E$, (where σ is the conductivity) it is not difficult to show that

$$\mu_q = (1/nq)\sigma \quad (16)$$

In view of (10),

$$\mu_H = R\sigma \quad (17)$$

the change in symbolism will be readily apparent.

It happens that the mobilities determined by drift velocity experiments using equation (15) differ from those obtained from the Hall coefficient as in equation (17). Shockley has shown from Brillouin zone considerations that in general R and $(1/nq)$ should be related by

$$R = r/nq \quad (18)$$

where r has a value between 1 and 2; that the limiting case for $r = 1$ applies when the conduction mechanism is highly degenerate; and that for spherical energy surfaces with lattice scattering dominating, r may be replaced by $3\pi/8$.

When the condition of the theory that assumes the crystal to be considerably longer than it is wide is not satisfied the short circuiting action of the end contacts on the Hall voltage can no longer be neglected. I. Isenberg and co-workers¹⁷ have advanced a theory wherein the error in such a measurement can be corrected. The detail of the theory is somewhat lengthy and will not be reproduced here; experimental verification is discussed in the article.

Thermomagnetic and thermoelectric effects must also be considered in electrical measurements of the type described here. Thermoelectric effects by themselves may falsify conductivity readings but the thermomagnetic effects are more troublesome in a combined set of readings, in

that they enter directly into the Hall voltage measurements. If the thermal gradients involved are not too great, the thermoelectric influence on the conductivity can be neglected. The Hall voltage, on the other hand, is frequently small and extraneous contributions to it could be relatively large. There is a technique whereby some of the troublesome extra voltages can be eliminated from the readings. This has the additional advantage that it also eliminates the commonly observed mismatch voltage resulting from the practical impossibility of positioning the Hall probes to contact the same equipotential plane.

Two of the thermomagnetic effects indicated result when a thermal gradient exists along the principal current axis (axis 3 in Figure 1). Due to this gradient a thermal current is produced in the sample. In the presence of the magnetic field a portion of the current carriers will be propelled toward one side of the sample, giving rise to a transverse voltage analogous to a Hall voltage. This is the Nernst effect. The "hotter" electrons, having higher energies (and hence higher velocities) will be selectively deflected in view of equation (6), and hence a transverse thermal gradient will be developed. The resulting thermal emf is called the Righi-Leduc emf.

Since the Righi-Leduc effect is a by-product of the Nernst effect, they can be considered jointly. Let N represent this combined thermal emf, let M represent any mismatch voltage present, and suppose V represents the sum of the Hall and the Etingshausen emf's. The Etingshausen effect will be considered shortly.

Ideally N can be considered independent of the direction of the primary current, and hence half of the difference of the voltages measured across the Hall probes for two directions of the primary

current is given by:

$$\frac{M + V + N - (-M - V + N)}{2} = M + V$$

Now, if the magnetic field is reversed, a third reading averaged with the second gives:

$$\frac{-M - V + N + (-M + V - N)}{2} = -M$$

The sum of these values (or the difference $M + V - (-M)$) then gives V .

The Etingshausen emf is a by-product of the Hall emf in much the same way that the Righi-Leduc emf is a by-product of the Nernst effect. It is generated because higher energy electrons are selectively deflected in a magnetic field. The Etingshausen field changes direction when the Hall field changes direction, and hence the above procedure is justified.

A technique for the removal of all three of these voltages has been described by Dauphinee and Mooser,⁸ provided the mismatch voltage can be eliminated. Further discussion of this method is deferred to Chapter III where the circuitry and apparatus are discussed.

Fortunately there are additional techniques whereby some of these thermal problems can be circumvented. Good thermal shielding minimizes the Nernst and Righi-Leduc effects, and symmetry in the leads equalizes the thermal emf's there. R. A. Smith¹⁹ has demonstrated that for a conductor roughly comparable to the samples examined here, the Etingshausen effect makes a contribution to the Hall voltage well outside the range of measuring accuracy used in this study. For this reason a more serious consideration of the Etingshausen effect will be omitted.

In practice it was found sufficient to determine the Hall voltage by taking half the difference between the two Hall potential difference readings obtained for two opposing magnetic field directions with

constant current direction.

General Conductivity Theory

Further theoretical considerations of the charge carrier density are necessary if the impurity densities, their ionization energies, and the position of the Fermi level are to be determined. To do this one requires a knowledge of the impurities present (the term impurities is intended to include imperfections of any kind that influence the conduction process, whether they act as donors or acceptors), whether there is more than one kind of donor or acceptor, and some knowledge as to what degree each affects the conduction process, etc. Since these conditions are uncertain in natural cassiterite at this time any theory must be given with some reservation.

It has become standard practice for authors of solid state text books to include discussions of temperature dependent parameters such as electron concentration, conductivity, and the like. Shockley,¹⁶ Smith,¹⁹ and Dekker²⁰ all present detailed discussions concerning the quantities of interest. A more thorough specific treatment of most of the theory of this section and related considerations has been compiled by Blakemore.²¹

The analysis used to study the data of Chapter IV incorporates the assumption that cassiterite is of the broad-band semiconductor class. More precisely, it has been assumed that:

- (a) there are N_d discrete donor sites per cubic cm, each E_d ev below the bottom of the conduction band,
- (b) the Fermi level (E_F) is several times kT below the bottom of the conduction band,

(c) there is a negligible contribution to the conduction either by holes or by electrons excited from the valence band in the temperature range of interest.

Some consideration will be given later to the possibility of limited compensation due to acceptor states, but fundamentally these conditions are taken as true.

In general the Fermi-Dirac probability function

$$f(E) = \left\{ 1 + \exp[(E - E_F)/kT] \right\}^{-1} \quad (19)$$

will be employed. With the zero of energy referred to the bottom of the conduction band, the distribution of allowed electron states takes the form

$$N(E) = \left\{ \begin{array}{ll} 4\pi(2m^*)^{3/2} h^{-3} E^{1/2}, & \text{if } E > 0 \\ 0 & \text{, if } E \leq 0, \text{ but } E \neq E_d \\ N_d & \text{, if } E = E_d \end{array} \right\} \quad (20)$$

where m^* represents the effective electron mass. Note that $N(E)$ defined in this way includes the factor 2 to allow for spin degeneracy in the conduction band.

At a given temperature the conduction electron density is then

$$n = \int_0^{\infty} N(E) f(E) dE$$

or

$$n = 4\pi(2m^*)^{3/2} h^{-3} \int_0^{\infty} E^{1/2} \left\{ 1 + \exp [(E - E_F)/kT] \right\}^{-1} dE \quad (21)$$

According to condition (b)

$$\exp [(E - E_F)/kT] \gg 1$$

and equation (21) may be written to good approximation as

$$n = 4\pi(2m^*)^{3/2} h^{-3} \int_0^{\infty} E^{1/2} \left\{ \exp [(E_F - E)/kT] \right\} dE$$

This integrates to

$$n = 2(2\pi m^* kT)^{3/2} h^{-3} \exp(E_F/kT) = N_c \exp(E_F/kT) \quad (22)$$

Equation (22) accounts for all electrons above the bottom of the conduction band. Those of interest below the conduction band are bound to donor states according to

$$n_d = \int_{-\infty}^0 N(E) f(E) dE = N_d \left\{ 1 + \exp [(E_d - E_F)/kT] \right\}^{-1} \quad (23)$$

Using the condition for charge neutrality

$$n + n_d = N_d \quad (24)$$

equations (23) and (24) combined simplify to

$$n = N_d \left\{ 1 + \exp [(E_F - E_d)/kT] \right\}^{-1} \quad (25)$$

Eliminating $\exp(E_F/kT)$ between (22) and (25) results in

$$n^2 = (N_d - n) N_c \exp(E_d/kT) \quad (26)$$

Under conditions of temperature for which

$$n \ll N_d$$

equation (26) has the approximate solution

$$n = (N_c N_d)^{1/2} \exp(E_d/2kT) \quad (27)$$

Equations (22) and (27) can be used to determine both E_F and E_d . For example, recalling that

$$n = r/Rq$$

when $RT^{3/2}$ is plotted on a logarithmic scale versus $1/T$, the slope of a straight line portion of the resulting curve is E_F/k as can be seen from equation (22). Note that an apparent straight line portion in this curve implies that in the temperature region considered the Fermi level is essentially independent of temperature. Similarly, the slope of a straight line portion on a $RT^{3/4}$ versus $1/T$ graph is $E_d/2k$, according to equation (27). Once E_F is calculated, since n may be assumed known at some particular temperature in the range of interest, equation (22) can be used to determine N_c ; and subsequently, since π , k , and h are known constants, m^* can be determined from this value. For convenience N_c may be written in the form

$$N_c = 2(2\pi mkT)^{3/2} h^{-3} (m^*/m)^{3/2} T^{3/2}$$

or

$$N_c = 4.831 \times 10^{15} G^{3/2} T^{3/2} \quad (28)$$

where

$$G = m^*/m = 3.499 \times 10^{-11} N_c^{2/3} (1/T) \quad (29)$$

and m is the free electron mass.

When the values of E_F , E_d , and N_c are known, N_d may be determined from the relation

$$E_F = E_d/2 + (kT/2) \log_e(N_d/N_c) \quad (30)$$

which may be obtained by equating equations (22) and (27), taking the natural logarithm of both sides of the resulting equation, and then solving for E_F .

The values quoted for effective mass and donor densities have been obtained in this way. Obviously calculations of this nature do not admit to high degrees of accuracy, but they have merit in establishing orders of magnitude.

In the event there is compensation through the action of traps or acceptor levels that lie well below the donor levels, the Fermi level will be found to lie closer to the donor levels, and a new approximation to equation (27) must be made.

Suppose that a fraction γ of the electrons supplied by donors go to fill up states where they are so tightly bound that below a particular temperature this number of electrons can be considered essentially constant. This is equivalent to saying that there are γN_d levels at which electrons contributed by major donors may be trapped. For this condition the conduction electron density will be given by

$$n = N_d \left\{ 1 + \exp \left(\frac{E_F - E_d}{kT} \right) \right\}^{-1} - \gamma N_d \quad (31)$$

instead of (25). If γN_d is an appreciable fraction of the total number of electrons so that

$$\gamma N_d \gg n$$

then to the first approximation

$$\gamma = \left\{ 1 + \exp \left[\frac{(E_F - E_d)}{kT} \right] \right\}^{-1} \quad (32)$$

Eliminating $\exp(E_F/kT)$ between equations (22) and (32) the results simplify to

$$n = \left[\frac{(1 - \gamma)}{\gamma} \right] N_c \exp(E_d/kT) \quad (33)$$

Equating (22) and (33) and solving for E_F gets

$$E_F = E_d + kT \log_e [(1 - \gamma)/\gamma] \quad (34)$$

It remains to consider equation (17) in light of equations (22), (27), and (33). An expression for σ is often written as

$$\sigma = \sigma_0 \exp (-\Delta E/2kT) \quad (35)$$

where σ_0 is a coefficient depending on what value μ_H has, and on which of the preceding expressions for n is most appropriate. In view of the previous development, it is obvious that the application of this expression must be approached with caution. Depending upon whether assumptions leading to equation (27) or equation (33) are valid, the factor $-\Delta E$ will give either the donor activation energy or twice the donor activation energy. Furthermore the coefficient σ_0 will have a temperature dependence based upon the type of scattering mechanism. At high temperatures (in the intrinsic range which was not covered in the current study) the validity of equation (35) for determining the forbidden energy gap for simple semiconductors is better established.

There are a number of other cases aside from those leading to equations (27) and (33), but these considerations will prove adequate for the analysis indicated in Chapter IV. Some interesting cases are discussed by R. A. Smith¹⁹ where the nature of the acceptor levels involved is known.

CHAPTER III

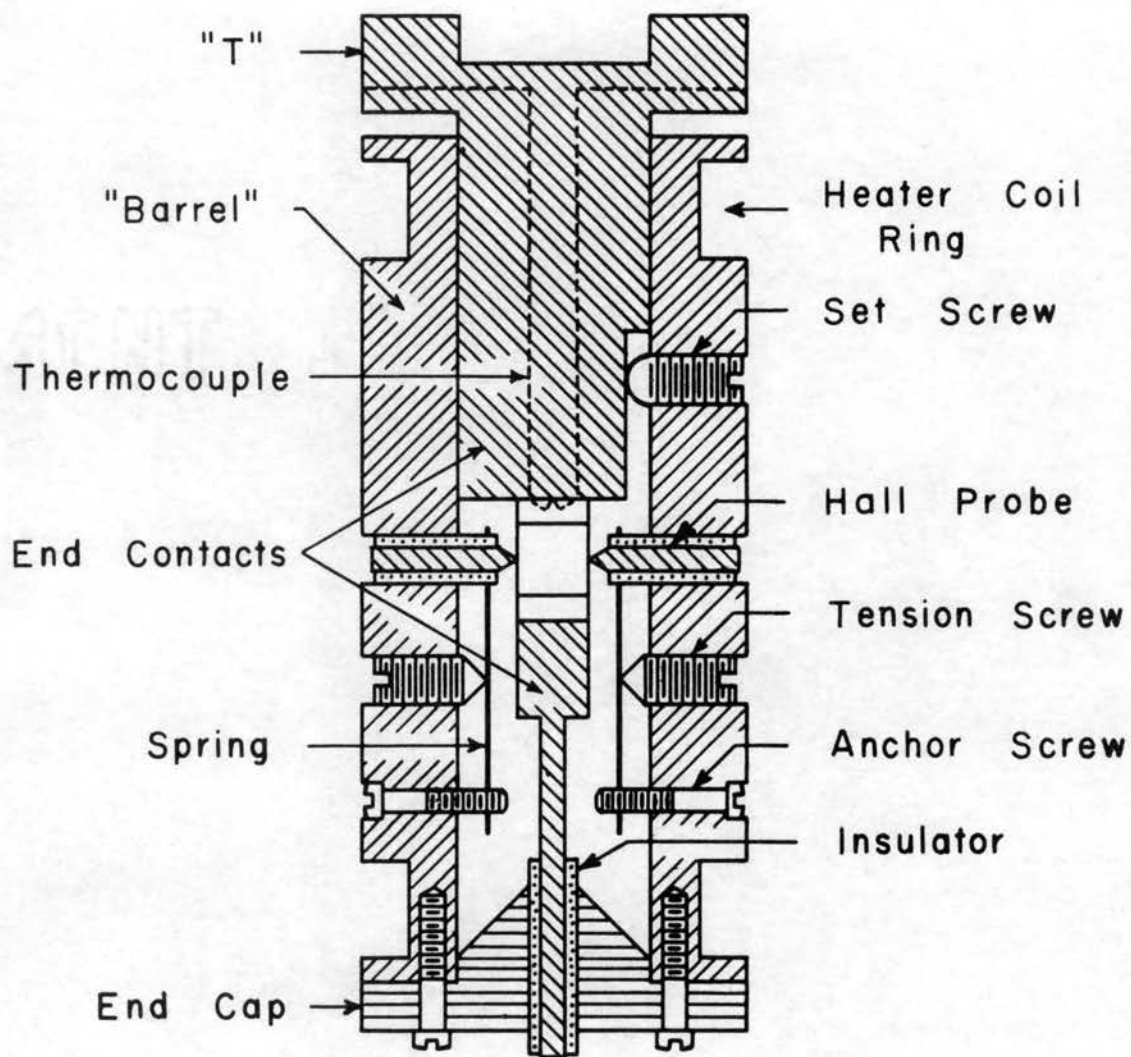
APPARATUS, EXPERIMENTAL TECHNIQUES, AND CRYSTALS

The Crystal Holder

Stringent requirements were placed on the design and materials used in building the crystal holder. Foremost of these requirements are as follows: First, an adjustable sample holder capable of accommodating various sizes of crystals was required. Second, spring activated contacts were necessary in order that thermal expansion and contraction be compensated. Third, all materials used in the proximity of the crystals were to be relatively non-magnetic to facilitate Hall effect measurements. Fourth, it was desirable that all materials used be suitable for the full temperature range of investigation in order that only one crystal holder need be built. Fifth, the size of the crystal holder had to be kept small in order that high homogeneous magnetic fields might be obtained. The manner in which these requirements were satisfied will be indicated in the description that follows.

The model selected was built in three parts, (Figure 2), a solid "T" with circular cross section, a hollow cylinder or "barrel", and an end cap.

A depression was cut in the top of the "T", and this was fitted with, and silver soldered to the bottom end of a stainless steel can (Figure 4). This "T" served as one end contact to the crystal as well



(1" = 1/2")

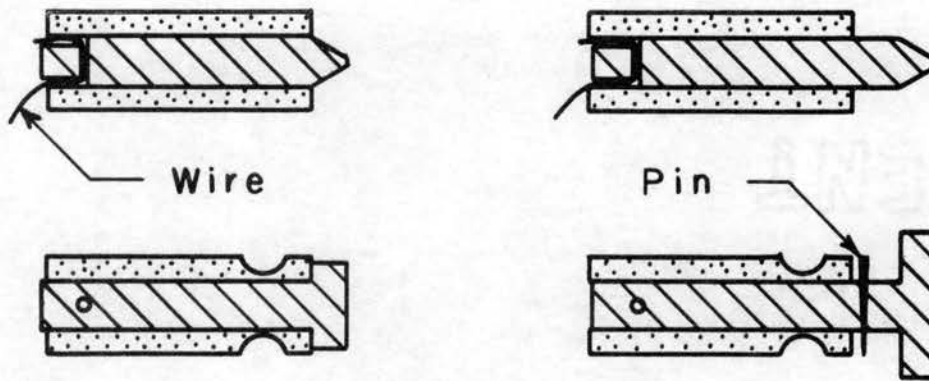
Figure 2. Cross section of crystal holder

as affording thermal contact to the can. A shallow groove was cut across the lower end of the "T" to help position and hold the crystal. Two small holes were drilled in the "T" (illustrated by the broken lines in Figure 2) to allow passage of thermocouple wires from the outside of the can to the interior of the crystal holder, the junction being imbedded in a shallow hole in the "T" near the end of the crystal. Electrical contact to the sample holder was avoided by use of Sauereisen cement at the junction and ceramic tubing on the leads. A set screw groove cut vertically along one side of the "T" satisfied alignment requirements; the set screw, serving as a support for the rest of the crystal holder, was contained in the "barrel".

The "barrel" contained both the Hall and potential difference (P.D.) probes. For insulation each of these probes was turned to fit into a one-eighth inch (oversize 3mm) glass tubing sleeve (Figures 3-a, 3-b). One-eighth inch holes were then drilled in the "barrel" to accommodate these sleeves, leaving each probe with one degree of freedom. The relative vertical position of the Hall probes and the separation of the P.D. probes was thus fixed. The P.D. probes, not shown in Figure 2, occupied positions in the crystal holder indicated by the two strips on the crystal.

By moving the "barrel" up or down on the "T" crystals with lengths between 7.5 mm and 15 mm could be mounted, being limited in the smaller value by the P.D. probes and in the larger value by the length of the crystal holder itself. Crystals of width up to 7 mm and thickness up to 3 mm could be accommodated by lateral adjustment without modification in the probe system, being limited in smaller dimensions only by inadequate crystal strength.

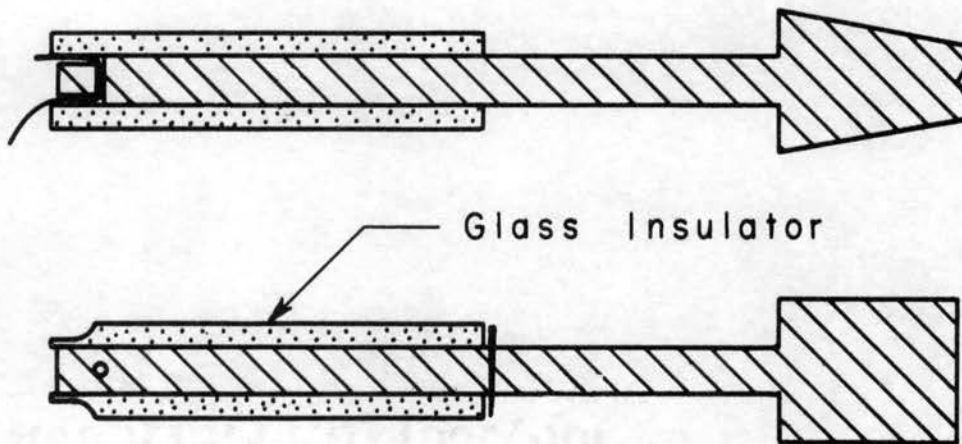
(1" = 1/4")



(a) Hall Probe

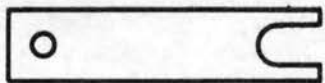
(b) P. D. Probe

(1" = 1/4")

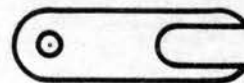


(c) Lower End Contact

(1" = 1/2")



(d) Probe Spring



(e) Contact Spring

Figure 3. Crystal holder accessories.

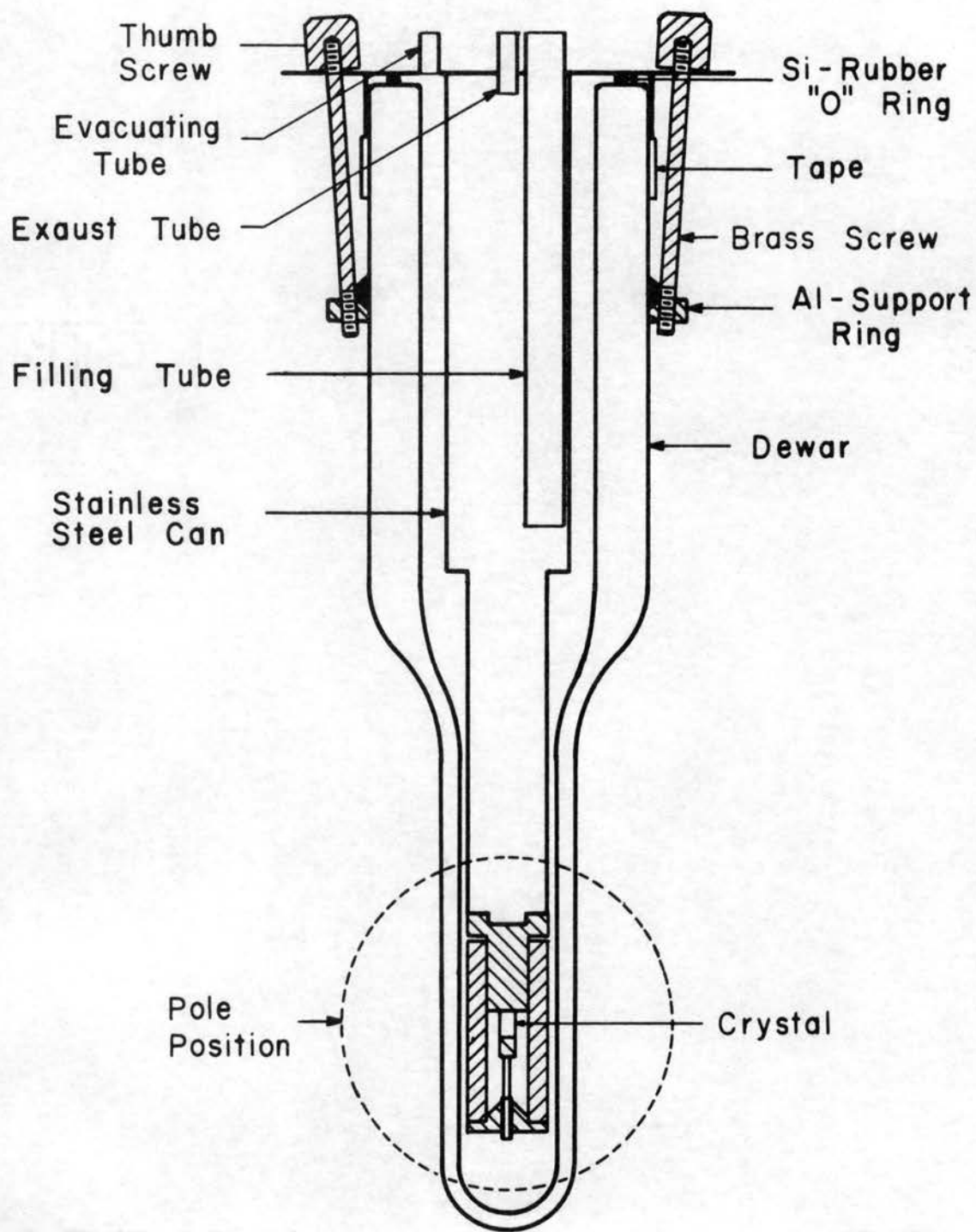
Each probe was spring actuated by a phosphor bronze leaf spring (Figure 3-d) that was slotted to fit into grooves ground in the glass insulating sleeves. These springs were all of the same size and thickness (0.010 inch). To facilitate lateral adjustment one end of each spring was drilled and tapped to accommodate an anchor screw. Tension was then applied by a screw midway between the anchor screw and the probe (Figure 2).

The lower end contact, similar to the probes and similarly insulated (Figure 3-c), was fitted into a one-eighth inch hole through the center of the end cap. It too was spring actuated by a phosphor bronze leaf spring (Figure 3-e). This spring was held in place by one of the end cap screws--tension being applied when the screw was tightened.

Figure 4 represents a cross section of the complete assembly. Part of the details have been omitted here for apparent reasons and a few comments about this figure will be necessary.

The lead-in wires were fed in through ceramic seals (not shown). This wire, #30 B. & S. gage size with fiberglass insulation, was supplied by the Thermoelectric Company. The way these wires were connected to the probes is indicated in Figure 3.

Two tubes opened into the vacuum chamber; only one is shown here. Provision was made for leveling by screws threaded through the lip at the top of the can, and these are not shown. To provide support for the assembly a wooden "saddle" was built for the magnet. In the center of this "saddle" a hole was drilled just large enough to pass the support ring (Figure 4), so that the weight of the assembly came to rest on the leveling screws. With proper adjustment the crystal occupied a position in relation to the pole pieces like that indicated in Figure 4.



(1" = 2")

Figure 4. Cross section of assembly.

The magnet used was a Varian Associates V4004 Electromagnet equipped with four-inch pole pieces. At full recommended operating capacity (8 amps) the field in a 1.65 inch air gap was measured to be 8,260 Gauss \pm 1% using a flip coil calibrated against a known standard.

The crystal holder parts, except the insulators and springs, were made of brass because of its suitable electrical, magnetic and thermal properties. Pyrex glass tubing was used to insulate the probes because of its resistance to thermal shock. Since it is relatively non-magnetic and an excellent thermal insulator at low temperatures, stainless steel was used to make the coolant can. The heater coils were wound with #24 B. & S. gage manganin wire, and a copper-constantan thermocouple provided sensitive temperature determination throughout the operating range.

Disadvantages. There are two principal disadvantages in the present design of the crystal holder. The first encountered was the formidable task of positioning the crystal in the crystal holder with a pair of tweezers - where it was difficult to see - while trying to clamp the crystal with the Hall probes. Clearly, considering the tolerances involved and the presence of wet contact material, this was not a desirable procedure.

Part of this difficulty was anticipated. Before the crystal holder was completed six 1/4 inch "peep" holes were drilled in the available spaces between the probes. These were threaded and fitted with plugs to preserve thermal shielding.

The problem of positioning was countered by building a sleeve in which the tweezers could be contained and locked, the outside dimension of which was nearly that of the inside of the "barrel" of the crystal

holder. This proved to be reasonably successful. Using a jewelers' eye loupe the Hall probes could be carefully positioned, and in this way the crystal held until the lower end contact was in place. This was done with the crystal holder inverted from the position shown in Figure 2.

The second disadvantage was inherent in the use of a fixed, two-probe system. Although the Hall probes were almost perfectly opposed, large mismatch voltages were often observed. Almost all of this could be credited to crystal irregularities, both in shape and composition. Above the ice point this did not present a great problem but at lower temperatures decreasing Hall voltages were soon obscured by increasing mismatch voltages. Accompanying this problem was the decreasing sensitivity of the Hall contacts and their eventual failure. It seems possible that the relative rates of expansion of cassiterite and brass may have been instrumental in contact failures at low temperatures although this has not been confirmed as yet.

At first sight, a three-probe contact system seems to be the logical answer to this difficulty; but until such time as good stable low resistance ohmic point contact can be made, contact failure at low temperatures will remain a limiting factor.

The problem of temperature stability at low temperatures was also not satisfactorily solved in the crystal holder just described. It was found impossible to maintain isothermal conditions at temperatures between 80°K and 273°K by a combination of liquid nitrogen cooling and simultaneous heating by the manganin heaters. All indications are that thermal contact between the coolant can and the sample holder attachment was insufficient to provide the desired control and that additional

thermal shielding of the crystal holder from the dewar walls is needed. (Improvements in these factors are under study prior to the design of new apparatus).

Some Hall effect measurements were attempted at fixed temperature points, principally liquid nitrogen and liquid propane boiling points, with only meager success. Combined with temperature drift problems was the erratic behavior or often complete failure of the Hall probes. Since geometry allowed larger area contacts for the P.D. probes and individual readings could be more quickly taken, values of low temperature electrical conductivity presented less of a problem.

The Circuit

Some of the difficulties involved in measuring temperature dependent parameters have already been pointed out. The requirement that the temperature be held constant during a given set of readings is difficult to satisfy when the time required may be long. This is particularly true when both the sample current and the magnetic fields must be reversed to eliminate spurious thermo-electric effects in the Hall voltage; and even this procedure fails to eliminate the Ettingshausen effect.

A measuring circuit designed to eliminate most of these difficulties has been described by T. M. Dauphinee and E. Mooser.¹⁸ The theory of operation, ably described in that article, will not be given in detail here. Figure 5, a modification of the circuit they used, provides for either A.C. or D.C. measurements through a simple switching procedure. Although the results reported in Chapter IV are based on standard two-probe D.C. Hall measurement techniques, both modes of operation are described since the feasibility of A.C. operation is still

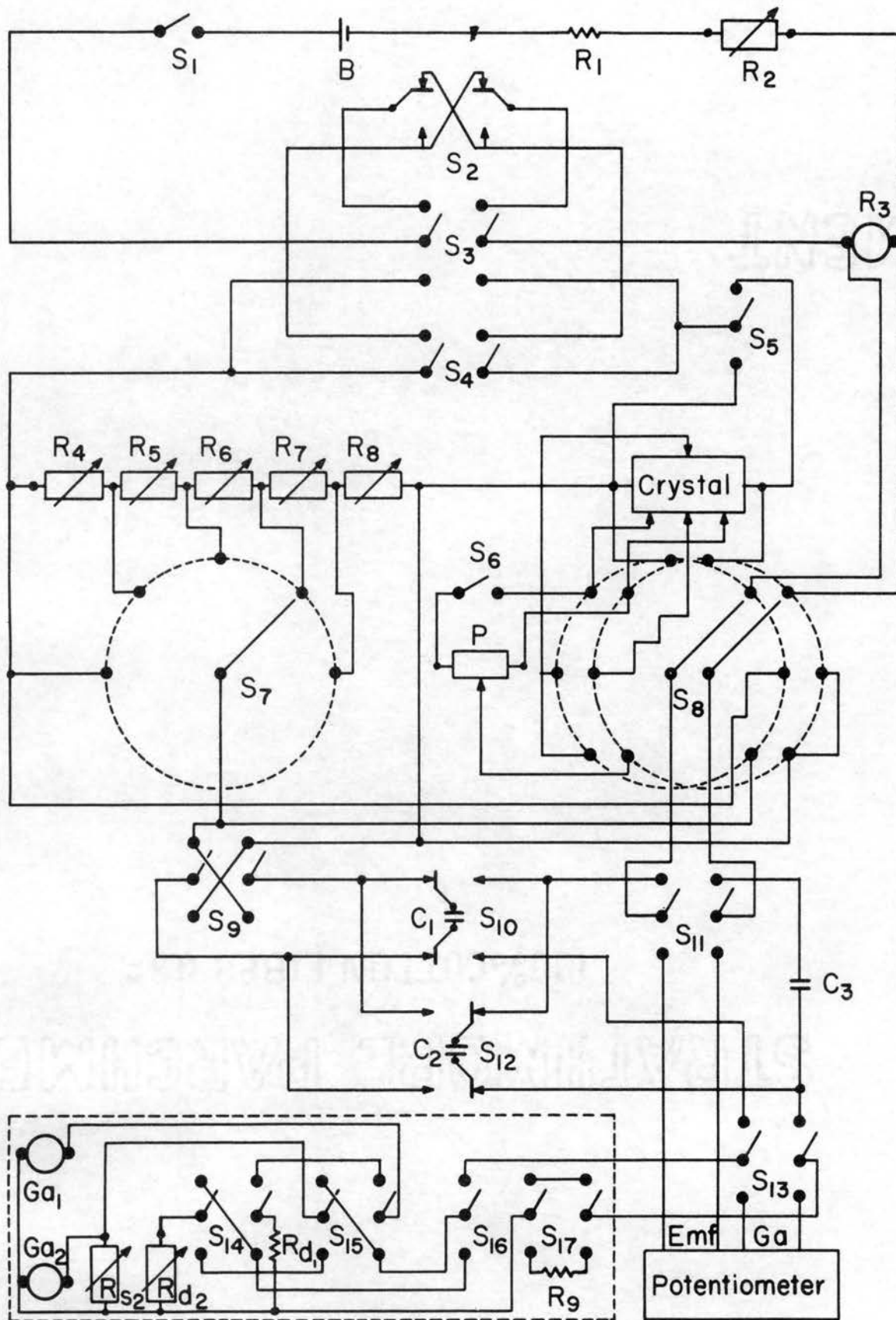


Figure 5. The circuit.

under study for future work.

With switches S_1 closed, S_4 and S_9 open, S_5 closed in the up position, and switches S_3 , S_{11} , and S_{13} closed in the down position, the circuit serves as a simple D.C. measuring circuit. Resistor R_1 is a current limiting resistor, and R_2 is for current regulation. Resistor R_3 is a standard resistor that can be replaced by an ammeter. Switch S_6 and potentiometer P were included in case a three probe system should be used. Switch S_8 is a voltage selector switch.

The portion of the diagram enclosed by dotted lines is a two galvanometer arrangement. Galvanometer Ga_1 was particularly suited for thermocouple measurements, and Ga_2 was a high sensitivity instrument-- necessary when high resistances were involved. When switches S_{14} and S_{15} are closed in the down position, Ga_1 is in the measuring circuit, while Ga_2 is shorted with its critical damping resistance R_{d2} . Conversely, with S_{14} and S_{15} closed in the up position, Ga_2 is in the measuring circuit while Ga_1 is shorted with its critical damping resistance R_{d1} . Galvanometer Ga_2 was shorted with a variable resistor R_{s2} , and a variable critical damping resistor R_{d2} was used. This was necessary if Ga_2 was to be kept matched to the measuring circuit since crystal resistances vary considerably with temperature and from crystal to crystal.

Switch S_{16} represents a tap switch that is closed in the up position when depressed, and closed in the down position when released. Switch S_{17} is a sensitivity switch, R_1 a meg-ohm resistor. With switch S_{13} either galvanometer could be used in either the A.C. or D.C. measuring circuits. A Leeds and Northrup K-2 potentiometer was used in the D.C. Circuit.

With switches S_1 , S_4 , and S_9 closed and switches S_3 , S_5 , S_{11} , and S_{13} closed in the up position, the circuit serves as an A.C. measuring circuit. This, basically, is the circuit described by Dauphinee and Mooser. Fundamentally this circuit is designed around a mechanical chopper composed of three double pole - double throw switches that can be driven at various speeds from a common shaft. One of these switches (S_2) is used to generate an A.C. square wave through the crystal and a series variable resistance, and the remaining two switches (S_{10} and S_{12}), when properly phased with the first, serve as potential comparitors. For example, switches S_{10} and S_{12} are wired to compare the voltage drop between the P.D. probes of the specimen with the voltage drop across reference resistors when the latter carry the same current. By shorting these switches with capacitors (C_1 and C_2) a charge proportional to the voltage measured is carried by each switch in each case, the difference in potential giving rise to a galvanometer deflection or a null balance when the voltages are the same. Switch S_7 allows a selection of resistances beginning with R_3 at (0 to 40 ohms) increasing through R_4 at (0 to 100K-ohms) with various values in between, and hence various voltages for comparison. With switch S_5 the specimen may be thrown out of the circuit, and a potentiometric measurement taken of the matching resistors used. The reversing switch (S_9) permits measurement of both positive and negative Hall coefficients. As pointed out by Dauphinee and Mooser, capacitor C_3 serves to block D.C. thermal voltages and when the chopper is operated at speeds in excess of 10 cycles per second the Ettingshausen effect does not have time to build up.

The selector-switch S_7 and resistor arrangement R_4 through R_8 is a modification of that used by Dauphinee and Mooser and has not yet been

thoroughly tested.

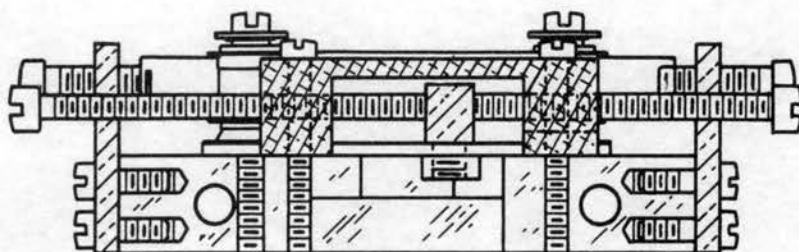
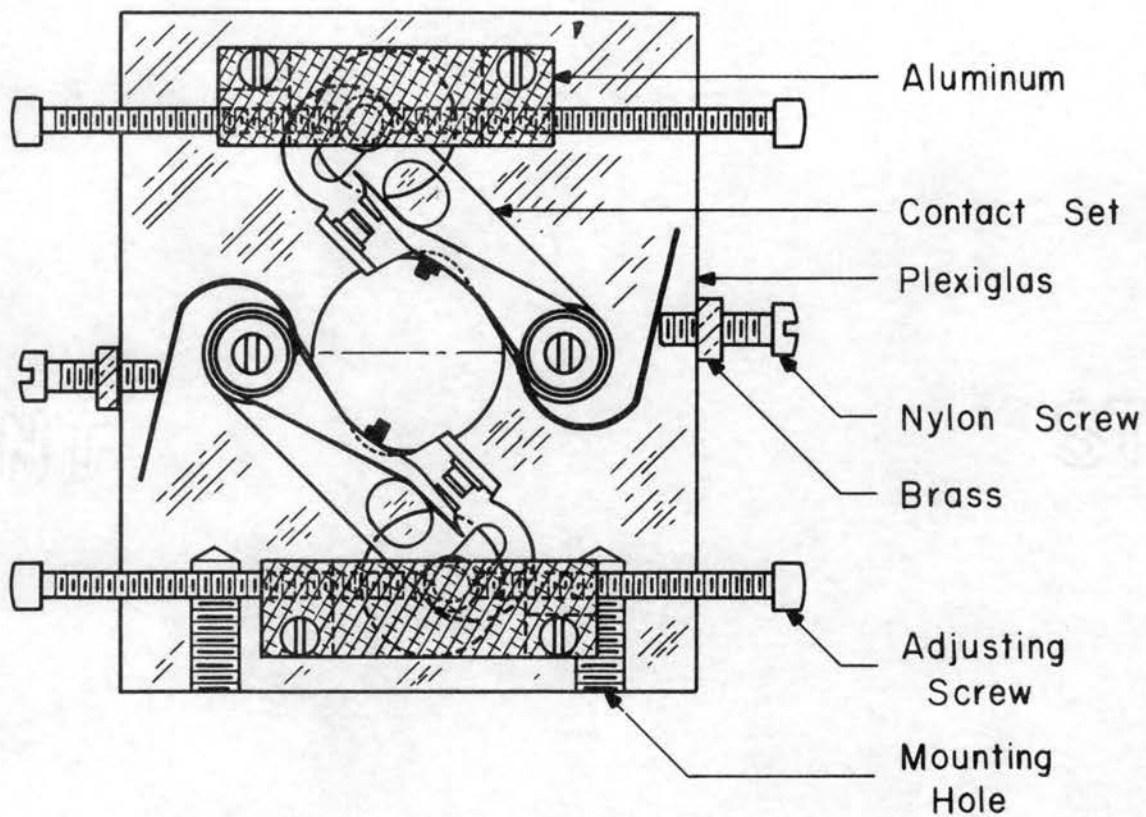
The mechanical chopper used by Dauphinee and Mooser has been described in another connection²² where it was used in a sensitive temperature control device.

A different chopper was built for the present investigation. To reduce the number of parts, commercial contact points were used. Those selected were Shurhit A-8 automobile ignition points. Using these as a basis for design, six sections like that shown in Figure 6 were built and mounted on a 1 ft. x 2 ft. metal plate 1/2 inch thick. Each section was aligned to a common shaft through its center, and each was actuated by a brass cam (Figure 6). Power was supplied by a Carter AC/DC gear reduction motor. Mechanically, the operation has been excellent but difficulty has been experienced in maintaining constant and continuous electrical contact at the points. Several possibilities for correcting this difficulty are still under consideration.

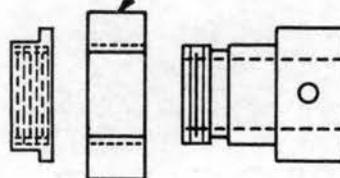
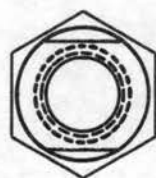
Special Temperature Control Procedures

In a sense there were two temperature ranges of investigation during the course of this study. One extended down from room temperature, the other up. Each was treated in a different way and will be considered separately in the order mentioned.

In view of the necessity of maintaining isothermal conditions during Hall effect measurements, which required readings for both field directions in order to cancel out the normal mismatch voltages across the Hall probes, several temperature stabilization methods were tried as previously described. The most successful procedure was carried out in the following manner: the coolant can was filled with and kept full



(1" = 1")



Cam

(1" = 1")

Figure 6. Chopper and cam.

of liquid nitrogen for two or three hours. Propane gas was then bubbled into the can, the liquid nitrogen being replenished until the can was about half full of solid propane. If this was done too quickly and the can warmed, it was refilled with liquid nitrogen until temperature stability was re-established.

When the residual liquid nitrogen had vaporized the temperature began a fairly slow steady increase toward room temperature with the propane acting as a large thermal mass stabilizer. Resistivity readings could then be taken at regular intervals.

A near "fix" could be obtained in this way at the propane point, but very little accurate Hall effect data was obtained there because of erratic contacts. Consequently, only a small amount of accurate Hall effect data has been obtained below 0° C.

Good results were obtained at room temperature, where water was used as a stabilizer, for both conductivity and Hall effect readings.

Above room temperature the slow but positive method of manually regulating the crystal holder heater current was employed. Although time consumptive, this method gave high precision and allowed very accurate readings for both conductivity and the Hall effect to be obtained.

Before low or high temperature runs were started a room temperature check of all values was made, and following each run a second check was made to compare with the first. Agreement was found to be very satisfactory.

The samples were maintained in a vacuum $\sim 10^{-2}$ mm of Hg by a roughing pump for all measurements.

Description of Samples

The samples studied have been cut from natural cassiterite crystals from Bolivia. Natural crystals are commonly obtained from intrusive hydrothermal igneous deposits where they have grown in association with other chemical elements, and consequently it is difficult to obtain a truly "clean" sample. A spectrographic analysis of the material used in this study indicated the principal impurities to be iron, aluminum and silicon. Even where apparently clean--or at least clear--material can be found it frequently contains a number of visible flaws, including cracks which contain microscopic mineral deposition and inhomogeneities, some of which have been found to be highly conductive. In general the samples used here were cut to minimize these imperfections.

Sample IX is clear with a number of inclusions and cracks. The cracks have been studied in some detail potentiometrically and found to exhibit preferential conduction along their length, though not in sufficient degree to detract greatly from bulk conduction.

Sample XVIII is mostly clear, has one dark end, a few small inclusions and no visible cracks.

Sample XIX varies from light yellow to light brown in different portions, has one clear corner, and has no visible fissures or cracks when these data were taken.

Sample SIA is transparent with a slight--nearly achromatic--grey tint, and otherwise contains no visible imperfections.

The mean dimensions of these four samples are listed in Table I. Both samples IX and XIX were re-cut after preliminary measurements to remove troublesome regions: an inhomogeneity in IX, and a small crack

along one edge in XIX; the final dimensions are given. Crystal XVIII was broken during an attempt to obtain high temperature Hall data; the dimensions presented here are those it had when the data of Chapter IV were taken.

TABLE I
CRYSTAL DIMENSIONS

Sample	Length (mm)	Width (mm)	Thickness (mm)
IX	8.20	5.02	0.96
XIX	10.17	4.60	1.12
XVIII	8.45	3.44	0.58
SIA	2.70	3.65	1.00

Crystal SIA is of uniform thickness, but it is otherwise irregular. The width and length given here are for the sample as it was mounted. That is, part of the more irregular portions were masked with contact material and the dimensions specified are for the unmasked portion of the crystal. The actual size is somewhat larger than this.

Contacts

All data were obtained using indium-gallium-mercury contacts. It was found that using roughly one part indium, two parts gallium, and one part mercury gave good noise free contacts to the crystals at and above room temperature. The contacts were made in the form of stripes rather than points and the stripe width and geometry could be nicely controlled when applied with a needle.

Preparation of Samples

The indium-gallium amalgam was most effectively removed by aqua regia. A specialized washing technique evolved from this, and the samples were cleaned using the following procedure:

1. Wash - aqua regia (3 parts HCl: 1 part HNO₃)
2. Rinse - distilled water - dried on filter paper
3. Wash - hydrofluoric acid
4. Rinse - distilled water - dried on filter paper
5. Wash - acetone
6. Rinse - methyl or ethyl alcohol - dried on filter paper.

Any material that could not be removed by this procedure, such as aquadag (initially a colloidal suspension of graphite in water), was found to be effectively removed by using a scouring powder, although this has the obvious disadvantage that it scratches the crystal surface.

Originally, the samples were cut from natural crystals with a diamond saw. Each was hand polished on paper that had been impregnated with alumina powder. Sample SIA, originally used by Northrip¹¹ in optical transmission studies, was further polished with Jewelers' rouge; clear or lightly colored samples that have been thoroughly polished in this manner are transparent.

CHAPTER IV

RESULTS

Much of this study has been concentrated in an effort to secure good noise-free ohmic contacts to the crystals in order that reliable data might be obtained. The contact materials used have already been discussed in Chapter III. Contact failures have in some cases necessitated remounting a crystal before a complete set of data could be obtained. The virtue of this difficulty lies in the fact that through remounting there are built-in checks against anomalies in crystal mounting procedures, and/or in reproducibility of the readings. It should be emphasized here, once again, that all results quoted in this chapter are the result of D.C. measurements as described in Chapter III.

Figure 7 is a plot of conductivity on a logarithmic scale versus $1/T$ for samples IX, XVIII, and XIX. Both the curves for IX and for XIX have been matched at room temperatures, and agreement has been found to be quite good for different mountings. For example, the difference between room temperature conductivity readings for different mountings of sample XIX was less than 3%, a difference attributed to stripe spacing measurements. No net curve shift was necessary to match the two segments of the curve for sample IX.

An interesting feature of these data is that in spite of widely differing values of conductivity at low temperatures the high temperature

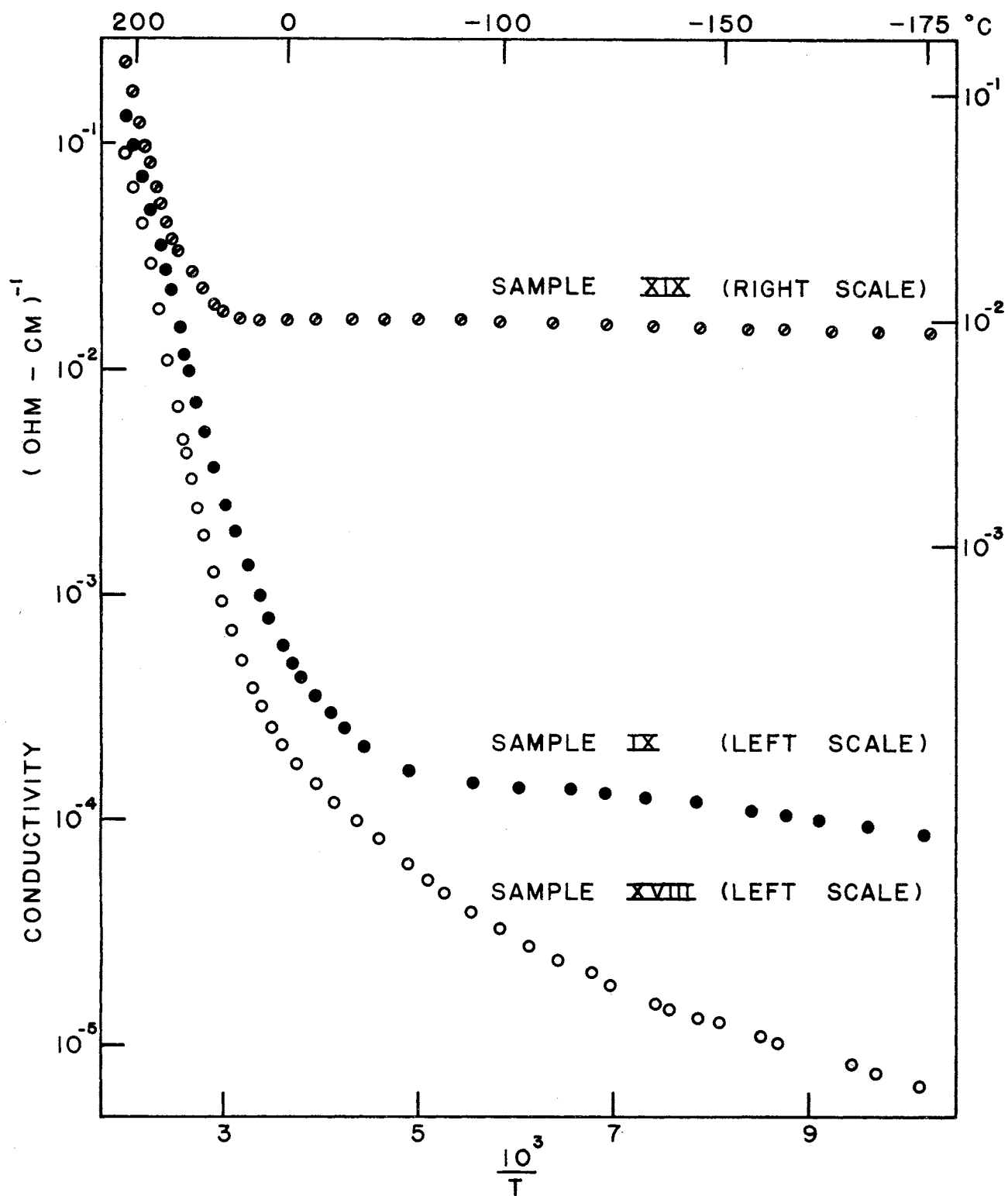


Figure 7. Conductivity Data as a Function of Temperature.

conductivity values differ very little. The high temperature curves of IX and XIX were so nearly the same that it was necessary to plot datum points for XIX to a displaced scale in order that these two curves not be superposed. Moreover, the slopes of the respective curves are very nearly the same. Values of ΔE calculated directly from equation (35) vary slightly depending on what portions of the curves are most critically analyzed. Possibly the most representative value in the higher temperature range - where the slopes are most nearly equal - is 0.72 ev. Low temperature values of $\Delta E \sim 0.01, 0.05, \text{ and } 0.005$ ev have been calculated for IX, XVIII, and XIX, respectively, again using equation (35). Room temperature conductivity values $\sim 10^{-3}, 10^{-4}, \text{ and } 10^{-2}$ (ohm-cm)⁻¹ were obtained for the three samples in the order just mentioned.

Figures 8 and 9 are graphs of conductivity and $RT^{3/4}$ plotted on separate logarithmic scales versus a common $1/T$ scale for samples IX and XIX, respectively. Each graph was plotted from high temperature data that can be readily correlated to Figure 7. The $RT^{3/4}$ curve has been plotted with the tacit assumption that equation (27) applies for the case in point. The slight departure of datum points (most notable in Figure 9 between 2.5 and 3.0 with respect to the $1/T$ scale) is the result of a retrace check after the samples were heated and maintained at high temperature for the order of a day or more. It is possible that this change was due to a slight diffusion of contact materials into the sample. There was an apparent change in the crystal surface in the proximity of the contacts that neither the adopted cleaning procedure nor surface polishing would remove.

As described previously, experimental difficulties at low

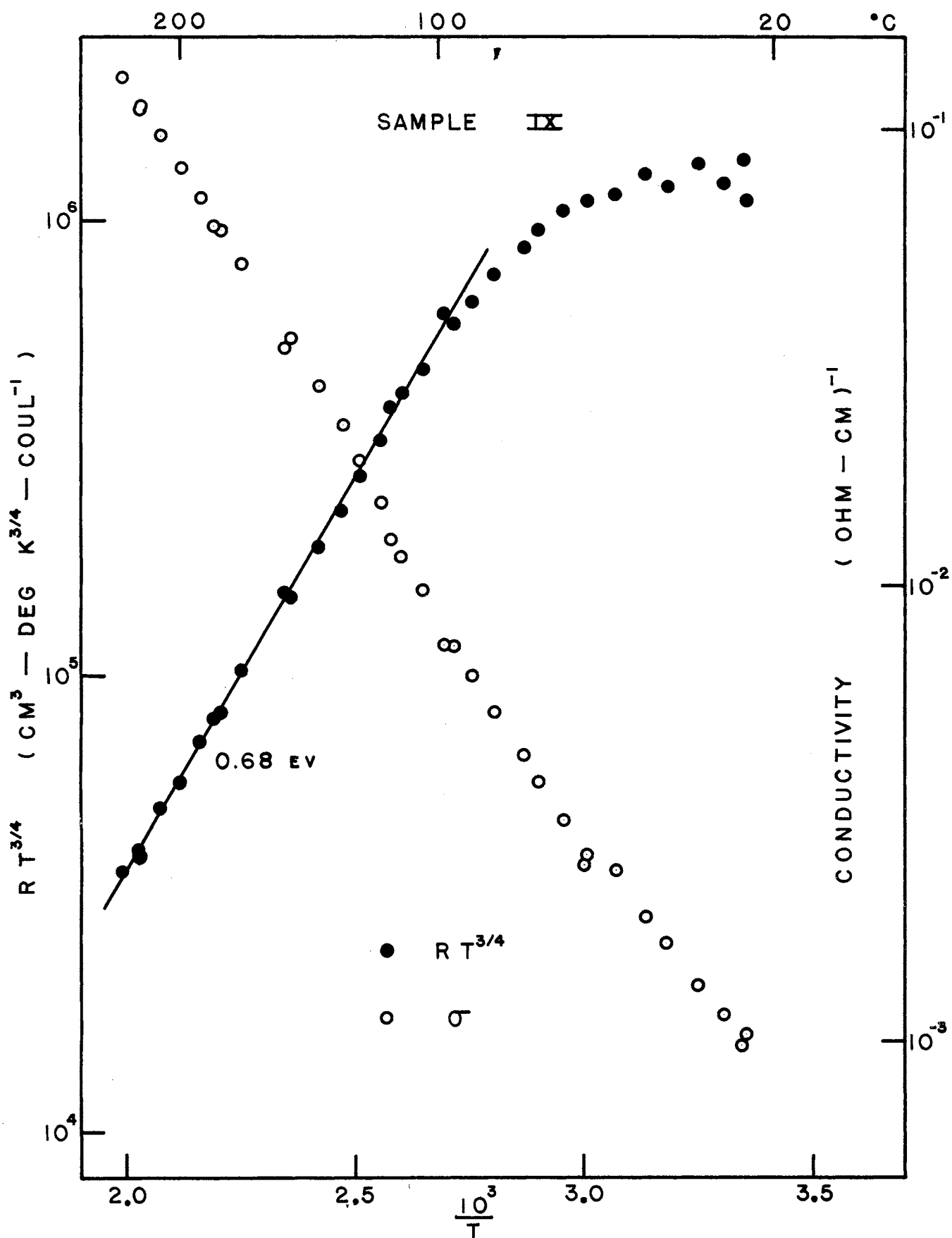


Figure 8. Hall Effect and Conductivity Data as a Function of Temperature for Sample IX.

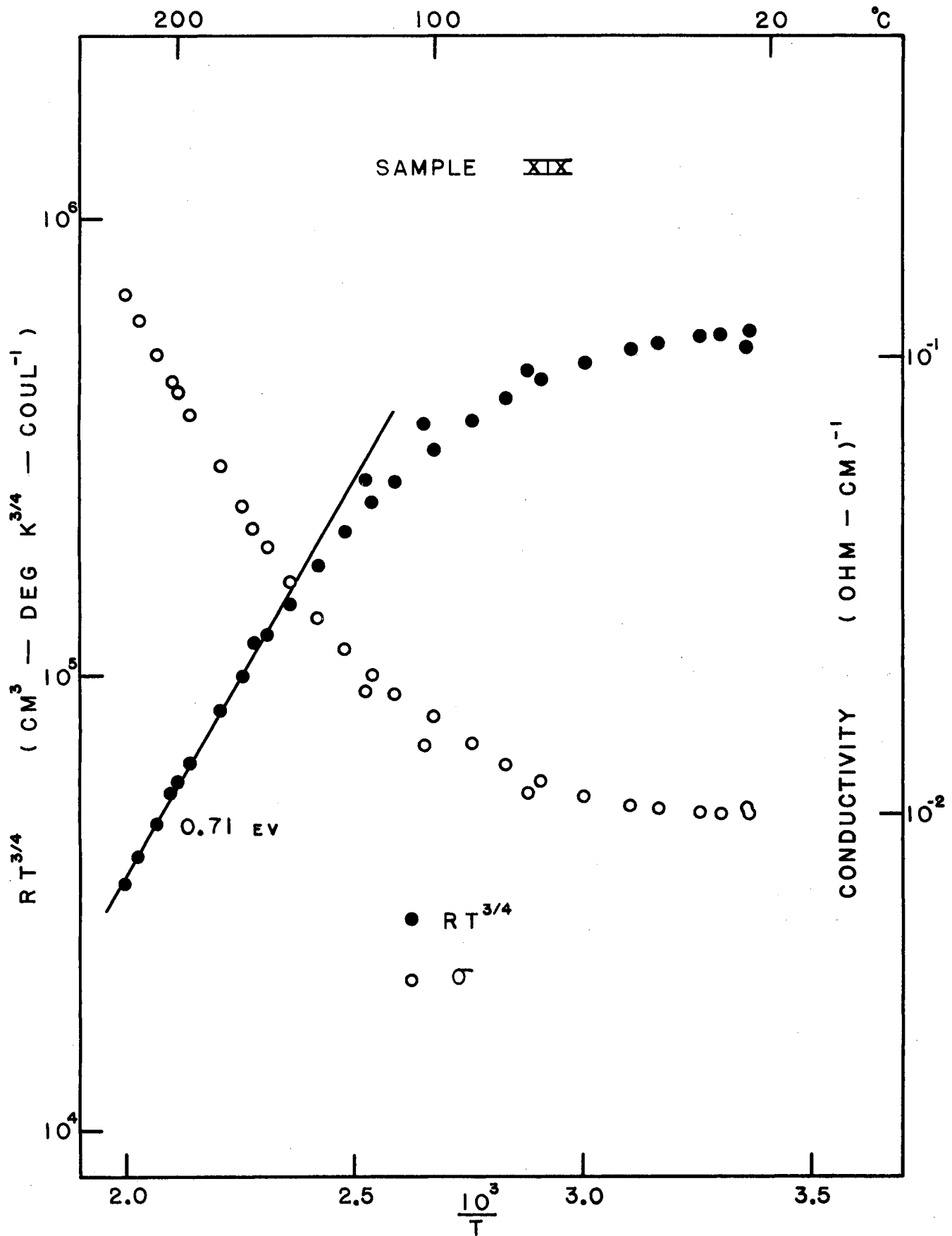


Figure 9. Hall Effect and Conductivity Data as a Function of Temperature for Sample XIX.

temperatures including noisy contacts and contact failure, temperature drift and lowered sensitivity due to high mismatch voltages, restricted the range of usable Hall data to temperatures above 0° C. Conductivity data were more readily obtained in that full stripes around the crystal were used and individual readings could be quickly taken.

Evaluations of activation energies from the $RT^{3/4}$ curves have been indicated in these two figures. If it is assumed that the charge carrier density is more correctly given by equation (33) than by equation (27), the calculated values of ionization energies become slightly less than half those given in the figures. However, reasonable degrees of compensation would still predict fractional effective masses, implying that the conclusion that the conductivity in cassiterite is broad-band in nature is still valid.

Charge carriers were found to be negative at all temperatures where the Hall effect was measurable. Low temperature thermoelectric power checks gave the same sign.²⁵ Room temperature values of n were determined using the $3\pi/8$ factor discussed earlier. Accordingly, the room temperature charge carrier densities obtained for IX, XVIII, and XIX are 4×10^{14} , 3.5×10^{14} , and $8 \times 10^{14} \text{ cm}^{-3}$, respectively.

Figure 10 gives $R\sigma$ or Hall mobility values as a function of temperature for samples IX and XIX. The temperature dependence for sample XIX is not too different from that to be expected for lattice scattering--as is that for sample IX at higher temperatures. However, the reason for the rapid dropoff at lower temperatures in the latter specimen is not apparent unless it has a connection with the presence of the flaws indicated earlier. An examination of the Hall mobility in sample XIX from about 170° C (2.26 on the $1/T$ scale) up to 227° C (2.00 on the

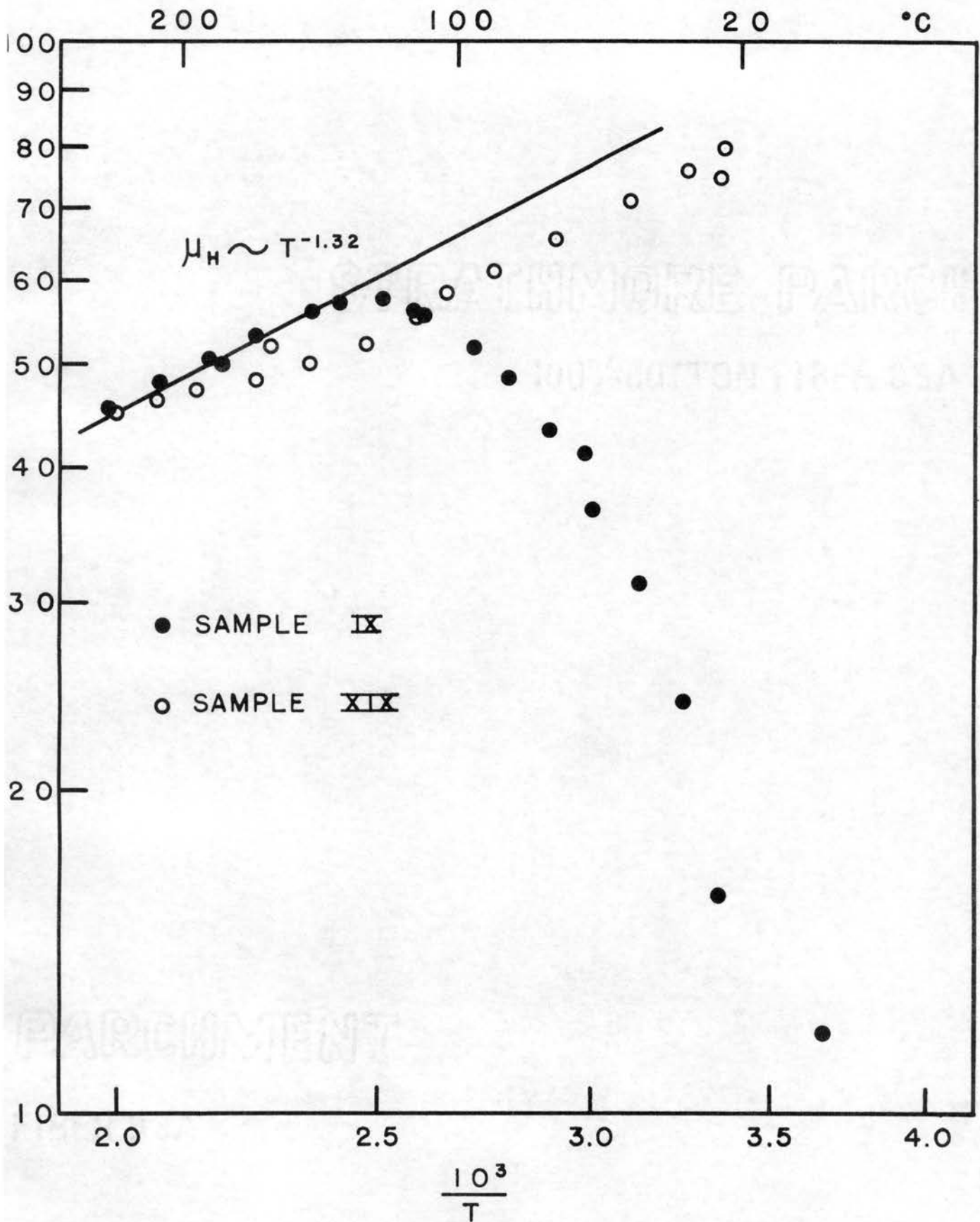


Figure 10. Hall Mobility as a Function of Temperature.

1/T scale) and back down to room temperature reveals a temperature variation more nearly as $R\sigma \sim 1/T$ than that given in the figure. This corresponds in part to the datum point departure previously referred to in Figure 9. The conductivity curve for sample XIX in Figure 7 does not show this effect since, because of the reduced scale used, these points were omitted.

Figure 11 represents some of the results obtained by Foex¹⁰ in a study of pressed powders. The technique he used to prepare the powder for this particular specimen was indicated in Chapter I. Foex attributed the break in the curve to the decomposition of some residual stannous oxide into stannic oxide and tin during the heating process. Values of ΔE have been given in the figure as calculated from a relation of the form of equation (35). The temperature slope to about 500° K is seen to be comparable to the values calculated from Figure 7. The difference between the intrinsic slope calculation and the optical energy gap (~ 3.5 ev) is not unnatural since thermal activation energy calculations depend on the ambient pressure and constituents. This was observed by Foex. A high temperature investigation of these effects on natural cassiterite is currently in the planning stage on this project.

Figure 12 represents an infrared transmission spectrum for sample XIX. Transmission studies have also been made on samples IX and XVIII with similar results. The prominent absorption dip occurs at about 3.07 microns, and the two satellites occur at about 2.98 and 3.15 microns. Soffer²³ found a similar absorption in rutile that he attributed to O-H stretching vibrations (i.e., hydroxyl radicals). Similar effects have also been observed in quartz.²⁴ The energy $h\nu$ for 3.1 microns is 0.40 ev.

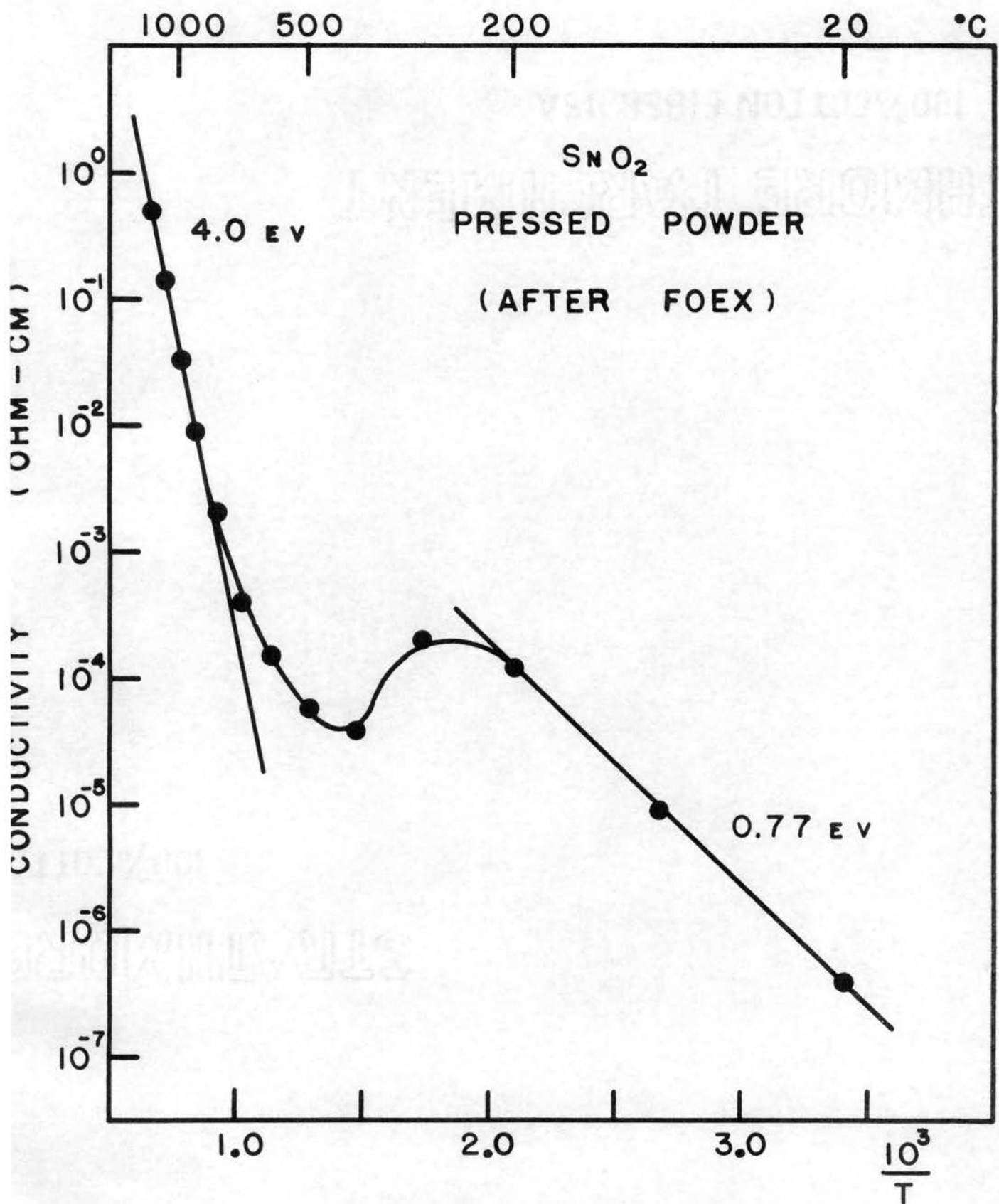


Figure 11. High Temperature Conductivity (Foex).

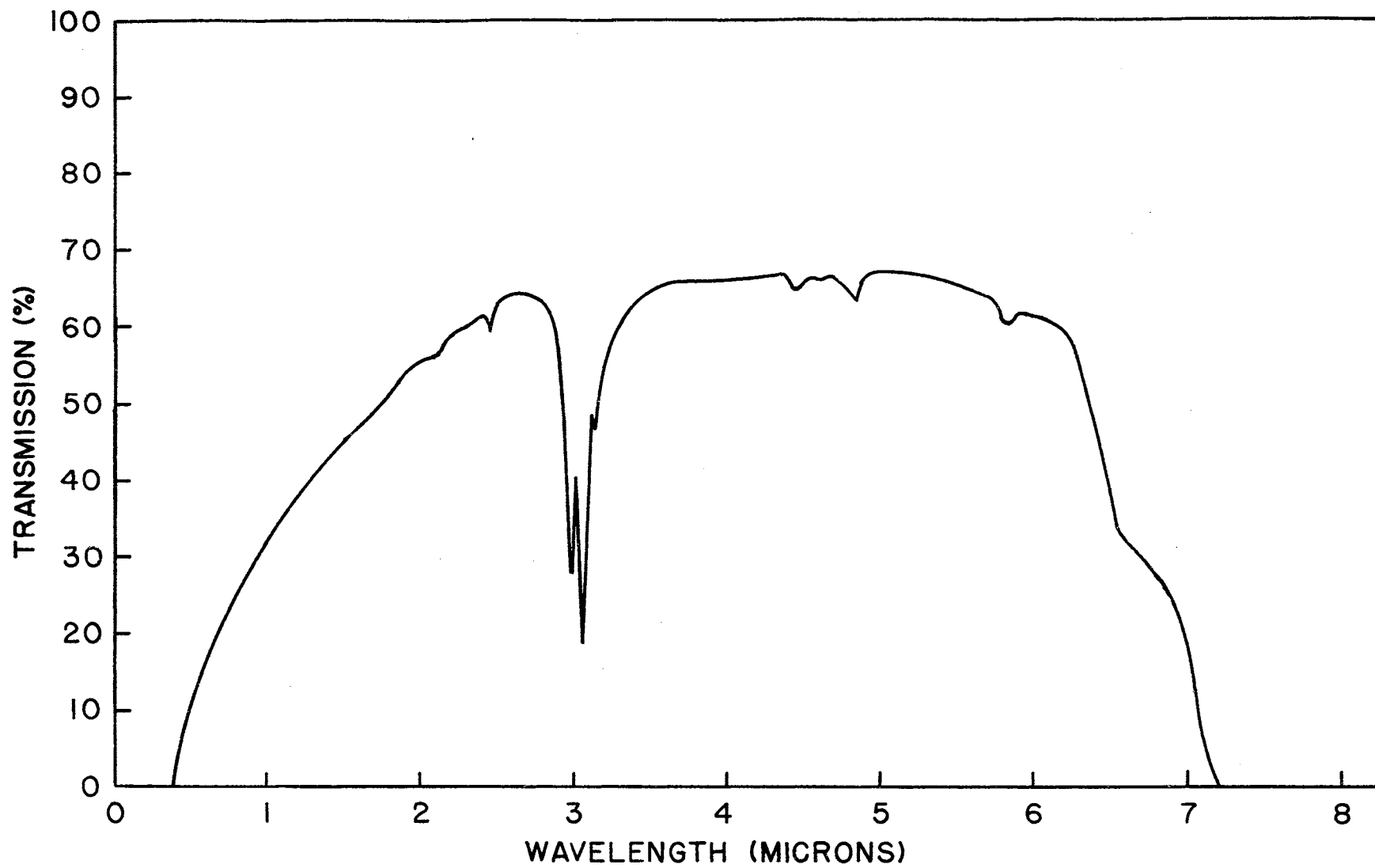


Figure 12. Transmission Spectrum of Sample XIX.

Summary

It seems somewhat more graphic to enumerate observations of particular interest and tabulate measured and calculated values.

Some of the more interesting properties of the data are as follows:

- (a) The high temperature conductivity curves for three samples have nearly the same slopes.
- (b) The higher the room temperature conductivity the less temperature dependence exhibited by the conductivity curves at low temperatures.
- (c) The higher the room temperature conductivity, the higher the temperature at which the steeper slope is taken up.
- (d) The conduction might be explained on the basis of two donor levels: One level 0.7 ev below the conduction band which controls the conductivity at high temperatures, and a second less-dense level near the bottom of the conduction band which governs the conductivity at lower temperatures.

Table II gives room temperature values of conductivity, charge carrier densities and Hall mobilities for the three samples already discussed. It also includes this information for a fourth sample, sample SIA. Major donor densities have been calculated wherever possible by using the approximate relation (30) developed in Chapter II. Effective mass values obtained through equation (29) are also given. Because of some degree of uncertainty in the latter values, particularly that for sample XIX, the effective mass is estimated at about 0.8 of the free electron mass.

TABLE II
MEASURED AND CALCULATED VALUES

Sample	IX	XVIII	XIX	SIA
Conductivity (ohm-cm) ⁻¹	1×10^{-3}	3×10^{-4}	1×10^{-2}	60
Carrier Density n (cm ⁻³)	4×10^{14}	3.5×10^{14}	8×10^{14}	1.2×10^{18}
Hall Mobility R (cm ² /volt-sec)	15	7	80	315
Donor Densities N _d (cm ⁻³)	1.1×10^{20}	not available	1.4×10^{20}	not available
Effective mass	0.65m	not available	1.0m	not available

CHAPTER V

CONCLUSIONS AND SUGGESTIONS FOR FURTHER STUDY

Perspective

It is not readily apparent, for reasons to be brought out in this section, just what impurities or imperfections are responsible for the results of Chapter IV. Some of the observations made during this study are of interest in that they in turn either suggest plausible explanations or rule out other possibilities, but the information immediately available is not adequate to draw well formed conclusions. From this view point then, this chapter is dedicated to an over-all perspective of the problem as it appears at this time.

As a first consideration, one is led to an analysis of the validity of the results.

In general the data do not appear to be wholly different from earlier measurements on the same type of material,¹¹ nor do the low temperature data appear in conflict with information available for some of the other oxides, as will become apparent. As previously indicated, the measurements show a high degree of reproducibility, internal consistency, and the differences between samples are about what should be expected for samples of differing impurity content.

Room temperature measurements taken by both J. Houston and J. Hurt²⁵ have indicated that conduction takes place primarily in the bulk of this material, with surface conduction estimated to constitute less than 10%

of the total in the most extreme case. The author also found that within the range of experimental error conductivity measurements were essentially independent of the width of the Hall probe contacts. (It is recognized, of course, that in using the described measuring technique the Hall contacts should be made as narrow¹ as possible). Probe contact resistances were usually about 25,000 ohms or higher. These findings seem to indicate that these samples have a highly resistive surface layer, and that the tacit assumption that conduction takes place largely in the bulk of the material is not unreasonable. It was also found by Hurt and the author that contact to the bulk of the material seemed dependent on sensitive spots on the surface, and this can be made to account for differences in contact resistance. To this extent the data seem reliable.

As a second consideration, it is desirable to seek a correlation between the results recorded here and those available from other studies of tin oxide.

A brief summary of studies made on films, sintered samples, and pressed powders of tin oxide has already been given in the Introduction. Published room temperature conductivity values for thin films and sintered samples are usually four or five orders of magnitude higher than the values recorded here, and electron concentrations are comparably higher. Reported activation energies at and near room temperatures, and below, center around values $\sim 0.02 - 0.05$ ev in some cases, comparable to those calculated for samples IX and XVIII here; while other values reported afford less good direct correlations. Hall mobilities are mostly within an order of magnitude of the values recorded here. Several of these investigators have suggested that the explanation of these

phenomena might be found in a detailed consideration of the stoichiometry; plausible explanations have been advanced based on a hydrogenic model as applied to either interstitial atoms or oxygen vacancies. This too may be an explanation of the low temperature conductivity and activation energy values obtained here, although it is not apparent on this basis why the low temperature conductivity slope for XIX is so small. Moreover, there is no immediate correlation between the hydrogenic model and the large activation energies at higher temperatures obtained in the present study.

As a third consideration, it is of interest to compare the results obtained here with those available for similar oxides, such as rutile (TiO_2) and zinc oxide (ZnO).

Because of the structural similarity between cassiterite and rutile it would seem most natural to examine data for rutile. However, in view of the evidence supplied by Frederikse and Hosler²⁶ that points to conduction in a narrow 3d band due to the atomic structure of titanium, such a comparison would be of questionable value.

Consider, then, some of the information available on zinc oxide.

H. Rupprecht¹ has shown that doping by the diffusion of hydrogen, zinc or indium into zinc oxide--in each case--gives rise to:

- (a) increased conductivity and electron density with increased diffusion,
- (b) a decreased temperature dependence of conductivity and electron density with increased diffusion, and
- (c) an increase of donors having low ionization energies (~ 0.034 to 0.06 eV) consistent with a hydrogen-like model.

An exception was noted for case (c) in that indium doped samples exhibited little or no temperature dependence in their conductivity or electron density values.

In a qualitative sense these observations seem to agree with the conductivity measurements below room temperature for the cassiterite samples studied here (Figure 7). Sample XIX has an apparent high density of impurities. Clear portions of samples IX and XVIII (in which measurements were taken) appear much the same, except for the visible flaws in sample IX. Potentiometric studies of IX, however, have indicated that there are some inhomogeneities in this sample aside from the visible flaws, that can be attributed either to non-stoichiometry, or to impurity content, so that sample XVIII might be classified as the purer of the two. High temperature conductivity curve comparisons with zinc oxide are less good, due in part perhaps to the differing degrees of degeneracy.

A. R. Hutson²⁷ observed similar effects in single zinc oxide crystals that were diffusion doped with hydrogen, zinc, and lithium. He found donor ionization energies ~ 0.05 ev for donor densities less than $5 \times 10^{16} \text{ cm}^{-3}$, again indicating that some impurities diffuse into zinc oxide crystals as donors having ionization energies comparable to those calculated from a hydrogenic model. On the other hand he also found that lithium doping gave rise to a "tailing off effect" in an electron density curve--an effect he attributed to compensation wherein a portion ($\sim 2\%$) of the lithium atoms acted as interstitial acceptors.

D. G. Thomas,²⁸ who was doing diffusion studies of zinc in zinc oxide crystals at about the same time, has advanced evidence that these effects, particularly the ionization energies, are to be attributed to interstitial zinc rather than to oxygen vacancies.

What interpretation can be made of these results is not apparent at the present time. It is important to remember that there is a considerable difference in the structure of zinc oxide (a wurtzite structure) and cassiterite (a rutile structure). It should also be noted that the measurements of ionization energies in zinc oxide were taken largely at and below room temperature, that heating of the samples appreciably above room temperature resulted in an outward diffusion of the interstitial materials in some of the cases,^{1,27} and that heating of the samples to about 550° C in air for only a few minutes was sufficient to remove essentially all of the interstitial zinc in the samples studied by Thomas.²⁸ Nevertheless, the fact that little or no outward diffusion of impurities was observed in the present investigation suggests the possibility that the impurity atoms may not occupy simple interstitial positions, and the possibility of conduction by electrons ionized from oxygen vacancies cannot be ruled out.

In view of the spectrographic analysis indicated earlier it seems natural to inquire into what possible roles the indicated impurities do play in the conduction process in cassiterite.

The presence of trivalent elements such as iron or aluminum immediately suggests the possibility of substitution--resulting in conduction by holes. This was not observed. Moreover, if appearance based on the samples studied here is used as an index of impurity concentration, the differences in electron densities are diametrically opposed to a simple substitutional hypothesis. The possibility that these impurities act as donors having low ionization energies--perhaps because they occupy interstitial position--is suggested by the diffusion studies of zinc oxide, but there appears to be no supporting evidence for such an assumption.

There is a type of information available on materials other than oxides that can be interpreted to suggest that the impurities here may play a more subtle role than the simpler ones just considered.

A number of people have taken interest in the role of gold and copper impurities in germanium and silicon. One of the more interesting of the earlier studies in this category was carried out for gold in germanium by Dunlap,²⁹ who coined the phrase "amphoteric impurity" because gold exhibits both an electropositive and an electronegative character in germanium. He gave evidence that gold is responsible for acceptor levels at 0.15 ev, 0.55 ev, and a donor level at 0.05 ev as measured from the valence band in each case. The energy gap in germanium is ~ 0.72 ev.

Woodbury and Tyler³⁰ reviewed the work done by Dunlap and other workers in the field and demonstrated a fourth level, an acceptor level, 0.04 ev below the conduction band. Also, they gave evidence that copper gives rise to three acceptor levels in germanium, two levels 0.04 ev and 0.32 ev measured from the valence band, and a third 0.26 ev from the conduction band.

E. A. Taft and F. H. Horn³¹ have found that gold produced a donor level 0.33 ev from the valence band in silicon. Silicon has an energy gap ~ 1.1 ev.

Dunlap²⁹ has also suggested, "It appears quite possible that a search among the transition elements, which have been shown to produce acceptor levels like gold in germanium, may also show up one or more donor levels for these elements."

Whether effects like those found for gold and copper in the elemental semiconductors germanium and silicon should be expected of some

of the elements, iron-aluminum-silicon-copper-lead-titanium, in an oxide like cassiterite appears uncertain at this time. A dominant impurity--iron--is a transition element, and the effects of copper in germanium have already been seen.

It is difficult to determine how to predict activation energies for interstitial impurities imbedded in a dielectric medium on a basis other than that provided by the hydrogenic model. In this connection, however, it is interesting to note that if the first ionization potential for free iron (7.83 ev) is divided by the dielectric constant of cassiterite (~ 24 at frequency 10^{12} cps according to the Handbook of Chemistry and Physics), a result ~ 0.33 ev is obtained. Similarly, dividing the second ionization potential for iron (16.16 ev) by the same dielectric constant gives a value ~ 0.69 ev. Beyond the striking agreement between these numbers and those obtained from high temperature data there is no readily apparent justification for making this type of calculation. Macroscopic analysis of microscopic phenomena is often misleading--the results may well be credited to chance.

The slight slope of the conductivity curve for sample XIX, corresponding to low temperatures, suggests that impurity band conduction might be in process there.

C. S. Hung, in an article by Hung and Gliessman,³² has advanced a quantitative technique by which impurity band conduction can be treated, and H. Fritzsche³³ has given the technique a more sound theoretical basis. An article by E. M. Conwell³⁴ is also of interest--both for a discussion on this subject and for a number of references listed. These investigators have found that the phenomena characterizing impurity band conduction include:

- (a) Little or no dependence of conductivity on temperature in the impurity band conduction range.
- (b) A marked temperature dependence of the Hall mobility during the transition from conduction in the ordinary bands to conduction in an impurity band.

Looking at Figure 7, condition (a) for sample XIX appears to be satisfied. But turning to Figure (10), condition (b) is not fulfilled. That is, if impurity band conduction is responsible for the leveling out of the conductivity curve starting at about 3.25 with respect to the $1/T$ scale, one looks for a marked change in the Hall mobility curve at this position in Figure (10). On the other hand, the Hall mobility curve for sample IX might seem to satisfy condition (b)--but then condition (a) is apparently violated. It may also be that the visible flaws in sample IX are responsible for the sharp dropoff in mobility.

It should be emphasized that the Hall data has been limited to temperatures largely above that of the laboratory due to experimental difficulties. Information at lower temperatures is incomplete.

Suggestions for Further Study

Most of the pursuits necessary for clarifying the particular problems discussed here are already being planned. The techniques necessary to grow artificial single crystals of cassiterite are being worked out. Work for a high temperature extension of conductivity measurements has already begun, and the effects of diffused trivalent and pentavalent impurities will be studied in the future.

In addition, it would be of interest to determine the effects of some of the transition elements in cassiterite, not only to satisfy the

question as to whether iron, copper, etc. produce an effect that has been measured here, but to see whether elements like gold would produce an effect like that observed in germanium and silicon. It is not inconceivable that a thermally stable material like cassiterite--in which donor or acceptor activation energies could be chosen somewhat at will--might find numerous applications at high temperatures.

In view of the difficulty in obtaining good contacts to cassiterite a thorough study of this problem would be desirable. Not only could such a study eliminate serious problems, but it could yield valuable information about the surface properties of the material. The latter information could lead to its use as a sensor or a catalyst for certain chemical reactions.

BIBLIOGRAPHY

1. H. Rupprecht, J. Phys. Chem. Solids 6, 144 (1958).
2. G. Bauer, Ann. Physik 30, 433 (1937).
3. A. Fischer, Z. Naturforsch 9a, 508 (1954).
4. K. Ishiguro, T. Sasaki, T. Arai and I. Imai, J. Phys. Soc. Japan 13, 296 (1958).
5. M. LeBlanc and H. Sachse, Physik Z. 32, 887 (1931).
6. P. Guillery, Ann. Physik 14, 216 (1932).
7. R. E. Aitchison, Australian J. Appl. Sci. 5, 10 (1954).
8. V. K. Miloslavskii, Optics and Spectroscopy (Russ. Trans.) 7, 154 (1959).
9. V. K. Miloslavskii and S. P. Lyashenko, Optics and Spectroscopy (Russ. Trans.) 8, 455 (1960).
10. M. Foex, Bull. Soc. Chem. France 11, 6 (1944).
11. J. W. Northrip II, Master's Thesis, Oklahoma State University, 1958 (Unpublished). Pertinent excerpts found in Annual Summary Report (1959), Office of Naval Research Contract No. Nonr-2595(01).
12. J. E. Hurt, Master's Thesis, Oklahoma State University, 1959 (Unpublished). Included as an Appendix in Annual Summary Report (1959), Office of Naval Research Contract No. Nonr-2595(01).
13. A. J. Belski, Master's Thesis, Oklahoma State University, 1960 (Unpublished). Included in the Annual Summary Report (1960), Office of Naval Research Contract No. Nonr-2595(01).
14. J. L. Marsh, Master's Thesis, Oklahoma State University, 1960 (Unpublished). Included in Technical Status Report No. 8 (1960), Office of Naval Research Contract No. Nonr-2595(01).
15. E. H. Hall, Amer. J. Maths. 2, 287 (1879); Amer. J. Sci. 19, 200 (1880).

16. W. Shockley, Electrons and Holes in Semiconductors. New York: D. Van Nostrand Co., Inc., (1950).
17. I. Isenberg, B. R. Russell and R. F. Greene, Rev. Sci. Inst. 19, 685 (1948).
18. T. M. Dauphinee and E. Mooser, Rev. Sci. Inst. 26, 660 (1955).
19. R. A. Smith, Semiconductors. New York: Cambridge University Press (1959).
20. A. J. Dekker, Solid State Physics. Englewood Cliffs, N. J.: Prentice-Hall, Inc., (1959).
21. J. S. Blakemore, Elec. Comm. 29, 131 (1952).
22. T. M. Dauphinee and S. B. Woods, Rev. Sci. Inst. 26, 693 (1955).
23. B. H. Soffer, Technical Report 140, Laboratory for Insulation Research, Massachusetts Institute of Technology, August, 1959.
24. G. Brunner, H. Wondratschek and F. Laves, Die Naturwiss. 46, 664 (1959).
25. Pertinent information given in the Annual Summary Report (1961), Office of Naval Research Contract No. Nonr-2595(01).
26. H. P. R. Frederikse and W. R. Hosler, NBS Report 6585 (1959).
27. A. R. Hutson, Phys. Rev. 108, 222 (1957).
28. D. G. Thomas, J. Phys. Chem. Solids 3, 229 (1957).
29. W. C. Dunlap, Phys. Rev. 100, 1629 (1955).
30. H. H. Woodbury and W. W. Tyler, Phys. Rev. 105, 84 (1957).
31. E. A. Taft and F. H. Horn, Phys. Rev. 93, 64 (1954).
32. C. S. Hung and J. R. Gliessman, Phys. Rev. 96, 1226 (1954).
33. H. Fritzsche, Phys. Rev. 99, 406 (1955).
34. E. M. Conwell, Phys. Rev. 103, 51 (1956).

VITA

Eugene Elmer Tolly

Candidate for the Degree of
Master of Science

Thesis: HALL EFFECT AND ELECTRICAL CONDUCTIVITY IN CASSITERITE CRYSTALS

Major Field: Physics

Biographical:

Personal Data: Born at Buffalo, Oklahoma, 1 April 1933, the son of Dalmer D. and Mary D. Tolly.

Education: Attended both elementary and high school at Buffalo, Oklahoma and graduated from high school there in May, 1951. Received the Bachelor of Science degree from Northwestern State College at Alva, Oklahoma in May, 1959.

Experience: Worked two years as a welder for the Oklahoma State Highway Department and served in the U. S. Army for two years before attending college.